ELSEVIER

Theoretical studies of self-organized criticality

Deepak Dhar*

Department of Theoretical Physics, Tata Institute of Fundamental Research, Homi Bhabha Road, Mumbai 400 005, India

Available online 2 May 2006

Abstract

These notes are intended to provide a pedagogical introduction to the abelian sandpile model of self-organized criticality, and its related models. The abelian group, the algebra of particle addition operators, the burning test for recurrent states, equivalence to the spanning trees problem are described. The exact solution of the directed version of the model in any dimension is explained. The model's equivalence to Scheidegger's model of river basins, Takayasu's aggregation model and the voter model is discussed. For the undirected case, the solution for one-dimensional lattices and the Bethe lattice is briefly described. Known results about the two dimensional case are summarized. Generalization to the abelian distributed processors model is discussed. Time-dependent properties and the universality of critical behavior in sandpiles are briefly discussed. I conclude by listing some still-unsolved problems.
© 2006 Elsevier B.V. All rights reserved.

Keywords: Abelian; Sandpile; Avalanches; Self-organized criticality; Dissipation; River networks

1. Introduction

These notes started as a written version of the lectures given at the Ecole Polytechnique Federale, Lausanne in 1998 [1]. I have updated and reorganized the material somewhat, and added a discussion of some more recent developments once before. The aim is to provide a pedagogical introduction to the abelian sandpile model and other related models of self-organized criticality. In the last nearly two decades, there has been a good deal of work in this area, and some selection of topics, and choice of level of detail has to be made to keep the size of notes manageable. I shall try to keep the discussion self-contained, but algebraic details will often be omitted in favor of citation to original papers. It is hoped that these notes will be useful to students wanting to learn about the subject in detail, and also to others only seeking an overview of the subject.

In these notes, the main concern is the study of the so-called abelian sandpile model (ASM), and its related models: the loop-erased random walks, the $q \to 0$ limit of the q-state Potts model, Scheidegger's model of river networks, the Eulerian walkers model, the abelian distributed processors model, etc. The main appeal of these models is that they are analytically tractable. One can explicitly calculate many quantities of interest, such as properties of the steady state, and some critical exponents, without too much effort. As such, they are very useful for developing our understanding of the basic principles and mechanisms underlying the general theory. A student could think of the ASM as a 'base camp' for the explorations into the uncharted areas of

*Tel.: +91 22 215 2971; fax: +91 22 215 2110.

E-mail address: ddhar@theory.tifr.res.in.

non-equilibrium statistical mechanics. The exact results in this case can also serve as proving grounds for developing approximate treatments for more realistic problems.

While these models are rather simple to define, and not too complicated to solve (at least partly), they are non-trivial, and cannot be said to be well understood yet. For example, it has not been possible so far to determine the critical exponents for avalanche distributions for the oldest and best known member of this class: the undirected sandpile model in two dimensions. There are many things we do not understand. Some will be discussed later in the lectures.

Our focus here will be on the mathematical development of these models. However, it is useful to start with a brief discussion of their origin as simplified models of physical phenomena.

2. Self-organized criticality in nature

It was the great insight of Mandelbrot that fractals are not mathematical curiosities, but that many naturally occurring objects are best described as fractals. Examples include mountain ranges, river networks, coastlines, etc. His book [2] remains the best introduction to fractals, for its clear exposition, evocative pictures, and literary style. The word 'fractal structure' here means that some correlation functions show non-trivial power law behavior. For example, in the case of mountain ranges, the irregular and rough height profile can be characterized by how $\Delta h(R)$, the difference of height between two points separated by a distance R, varies with R. It is found that

$$\langle [\Delta h(R)]^2 \rangle \sim R^x, \tag{1}$$

where $\langle \rangle$ denotes averaging over different spatial points at the fixed horizontal separation R, and x is some non-trivial power. When measured, the exponent x seems to not vary much between one mountain range and another.

In the case of river networks, the fractal structure can be characterized in terms of the empirical Hack's law [3]. This law describes how the catchment area of any particular stream in a river basin grows as we go down-stream along the river. If A is the catchment area, and ℓ is the length of the principal stream up to this point, Hack's law states that on the average A grows as ℓ^y, where y is some exponent, $y \simeq 1.6$.

In other examples the fractal behavior is found not in the spatial structure itself, but is manifest the power-law dependence between some physical observables. For example, in the case of earthquakes, the frequency of earthquake of total energy E is found to vary as E^{-z}, where z is a number close to 2, for many decades of the energy range. (This is the well-known Gutenberg–Richter law [4]). Recently, it was shown that the frequency of rain of a given intensity (amount of rain per unit area in a short time interval at the observation site) also follows a Gutenberg–Richter like power law for about five orders of magnitude of intensity [5].

An example in a similar spirit is that of fluid turbulence where an example of the fractal behavior is the way mean squared velocity difference scales with distance, or in the spatial fractal structure of regions of high dissipation [6].

A good understanding of these fractal structures should allow us to calculate the values of the critical exponents from physical principles, and not just tabulate them from experimental data. As the systems involved have many interacting degrees of freedom, techniques of statistical physics are expected to be useful in this.

Systems exhibiting long-ranged correlations with power law decay over a wide range of length scales are said to have critical correlations. This is because correlations much larger than the length-scale of interactions were first studied in equilibrium statistical mechanics in the neighborhood of a critical phase transition. In order to observe such critical phenomena in equilibrium systems, one needs to fine-tune some physical parameters (such as the temperature and pressure) to specific critical values, something rather unlikely to occur in a naturally occurring process such as the formation of mountains, where the actual shape is a result of competing processes of plate tectonics and erosion, and the external variables like the temperature have undergone big changes in time. The systems we want to study may be said to be in a steady state as while there is variation in time, overall properties are roughly unchanged over the time scale of observation. However, these systems are not in equilibrium: they are open and dissipative systems which require input of energy from outside at a constant rate to offset the dissipation. We define such states to be *non-equilibrium steady states*.

The term self-organized criticality (SOC) was first coined by Bak, Tang and Wiesenfeld (BTW) in their well-known paper in 1987 [7]. BTW argued that the dynamics which gives rise to the robust power-law correlations seen in the non-equilibrium steady states in nature must not involve any fine-tuning of parameters. It must be such that the systems under their natural evolution are driven to a state at the boundary between the stable and unstable states. Such a state then shows long range spatio-temporal fluctuations similar to those in equilibrium critical phenomena.

Bak et al. proposed a simple example of a driven system whose natural dynamics drives it towards, and then maintains it, at the edge of stability: a sandpile. It is observed that for dry sand, one can characterize its macroscopic behavior in terms of an angle θ_c, called the angle of repose, which depends on the detailed structure (distribution sizes, shapes and roughness etc.) of the constituting grains [8]. If we make a sandpile in which the local slope is smaller than θ_c everywhere, such a pile is stable. On such a pile, addition of a small amount of sand will cause only a weak response, but adding a small amount of sand to a configuration where the average slope is larger than θ_c, will often result in an avalanche whose size is of the order of the system size. In a pile where the average slope is θ_c, the response to addition of sand is less predictable. It might cause almost no relaxation, or it may cause avalanches of intermediate sizes, or a catastrophic avalanche which affects the entire system. Such a state is critical. BTW observed that if one builds a sandpile by pouring sand very slowly, say on a flat circular table (Fig. 1), one gets a conical shaped pile, with slope *equal to* θ_c. The system is invariably driven towards its critical state: it shows SOC.

The steady state of this process is characterized by the following property: sand is being added to the system at a constant small rate, but it leaves the system in a very irregular manner, with long periods of apparent inactivity interspersed by events which may vary in size and which occur at unpredictable intervals (Fig. 2).

A similar behavior is seen in earthquakes, where the build-up of stress due to tectonic motion of the continental plates is a slow steady process, but the release of stress occurs sporadically in bursts of various sizes. In the case of rain, the steady drive is provided by the sun's heat causing evaporation of water from the oceans, and the relaxation is the irregular burstlike events of rain. Many time-series like electrical noise, stock market price variations etc. show irregular bursts of large activity, and power-law tails in their power spectra ['1/f' noise]. We shall use the term SOC generally for non-equilibrium steady state of systems with many degrees of freedom, having a steady drive, but where the relaxation occurs in irregular burst (e.g. avalanches in sandpiles). There are many other sytems where SOC ideas have been applied, e.g. models of forest fires, biological evolution, brain activity, etc. Constraints of space, and lack of familiarity on my part
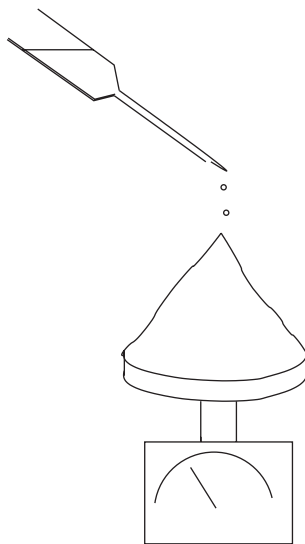

Fig. 1. A small sandpile on a flat circular plate attached to a weighing device, with grains added slowly from above.
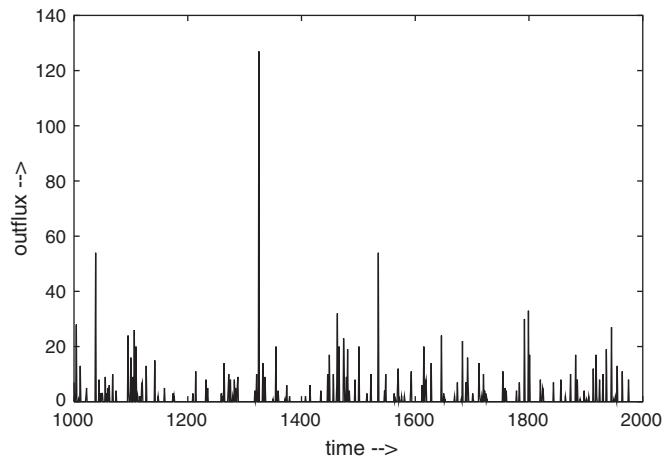
Fig. 2. A schematic representation of the outflux of sand as a function of time. The data shown was actually generated on computer by simulating the BTW model of sandpiles on a square lattice of size 100×100.

do not allow me to discuss all these here. For an overview of application of the SOC idea to different natural systems, see [9].

It has been argued that in fact self-organized systems are not really 'self-organized' reaching the critical point without any fine-tuning of parameters from outside, or very different from other critical systems, because here the driving rate is the parameter which is being fine-tuned to zero [10]. While the mechanism underlying SOC, and its relationship to conventional critical phenomena are important questions that need to be understood, let us not get involved in a discussion about the correct terminology at this stage, and agree to use the widely accepted term SOC, with the understanding that fine tuning to zero is not 'unnatural', is easily realized experimentally, and often occurs in nature.

3. Models of self-organized criticality

The first step in the study of SOC would be the precise mathematical formulation of some simple model which exhibits it. Such a system should have the necessary features of SOC systems: it should show *non-equilibrium steady state of an extended system with a steady drive*, *but irregular burst-like relaxations*, *and long-ranged spatio-temporal correlations*.

3.1. The BTW sandpile model

In their original paper [7], Bak Tang and Wiesenfeld also proposed a simple cellular automaton model of sandpile growth. The model is defined on a finite lattice, which we take for simplicity to be a cut-out portion of the two dimensional square lattice. There is a positive integer variable at each site of the lattice, called the height of the sandpile at that site. The system evolves in discrete time.

The rules of evolution are quite simple: at each time step a site is picked randomly, and its height z_i is increased by unity. If its height is then greater than a critical height $z_c = 4$, this site is said to be unstable. It relaxes by toppling whereby four sand grains leave the site, and each of the four neighboring sites gets one grain. If there is any unstable site remaining, it too is toppled. In case of toppling at a site at the boundary of the lattice, grains falling 'outside' the lattice are removed from the system. This process continues until all sites are stable.

Then another site is picked randomly, its height increased, and so on. To make the rules unambiguous, the toppling of sites which were rendered unstable during the same time step is defined to be carried out in parallel. It is easy to show that this process must converge to a stable configuration in a finite number of time steps on any finite lattice using the diffusive nature of each relaxation step (proof omitted).

The following example illustrates the toppling rules. Let the lattice size be 4×4, and suppose at some time step the following configuration is reached:

4	2	4	3
2	3	4	4
4	1	2	2
3	1	3	4

We now add a grain of sand at a randomly selected site: let us say the site on the second row from the top and the third column from the left. Then it will reach height 5, become unstable and topple to reach

4	2	4	3
2	3	5	4
4	1	2	2
3	1	3	4

$\longrightarrow$

4	2	5	3
2	4	1	5
4	1	3	2
3	1	3	4

,

and further toppling results in

4	3	1	5
2	4	3	1
4	1	3	3
3	1	3	4

$\longrightarrow$

4	3	2	1
2	4	3	2
4	1	3	3
3	1	3	4

.

In this configuration all sites are stable. One speaks in this case of an event of size $s = 4$, since there were four topplings. Other measures of event size are the number of distinct sites toppled (in this case also 4), the number of time steps needed (3 in this case), and the diameter of the affected area (3). Suppose that one measures the relative frequency of event sizes. A typical distribution would be characterized by a long power law tail, with an eventual cutoff determined by the system size L (see Fig. 3).

For readers who may like to write their own simulation program, we add some tips here: to get good statistics, one needs to minimize the finite-size effects. Avalanches that start near the boundary have a different statistics than those that start away from it (in bulk). In the limit of large sizes, the contribution of boundary avalanches to total goes to zero as $(1/L)$. In simulations, one gets much better convergence if the avalanches that start near the boundary are excluded from the data. Else, the distributions for different sizes converge very slowly with L even for small avalanche sizes. In Fig. 3, I used a cylinder of size $L \times L$, with periodic
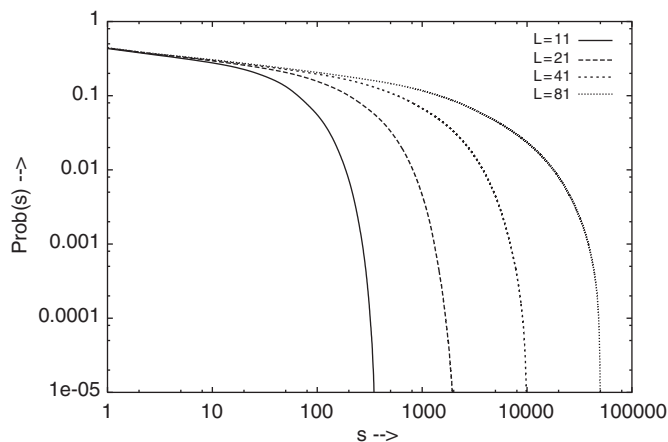

Fig. 3. The cumulative probability $\mathsf{Prob}(s)$ that an avalanche is of size greater than or equal to s, as a function of s for different lattice sizes. The curves were generated by simulation with over 10^6 events for each size of the lattice.

boundary conditions in the y-direction, and open boundary conditions in the x-direction. Particles were not added with uniform probability everywhere. The odd-numbered particles were added only along the middle ring away from the boundaries, with all sites on the ring equiprobable. Even-numbered particles were added anywhere on the lattice. Only avalanches resulting from the odd-numbered particles were used for determining the avalanche distributions. [We shall show later that this does not affect the answer.] Imposing cylindrical boundary conditions avoids corners, and consequent corrections to bulk behavior.

It is easy to think of variations of this model. One can work on a different lattice. Or choose a different rule for defining unstable sites: it seems more physically reasonable that the instability condition is on differences of heights between neighboring sites, and not on heights. One can choose different particle transfer rules: particles drop only to 'downward' sites, and not to 'upward' sites. The number of particles transferred in a toppling may depend on state of site before toppling. The thresholds for instability may not be same for all times, but reset randomly, and the particle transfer may also be random, etc. Many of these have been studied in literature, and some will be discussed in these lectures later.

While the BTW model is not a very good model of real sand, it is the paradigmatic model for studies of SOC. The analytical tractability of the model has led to a lot of interest in the model, and by now there is a fairly large amount of work dealing with this model. For recent reviews, see [11–14].

3.2. Loop-erased random walks

This is perhaps one of the simplest models showing burst-like relaxations. We consider a random walker on, say, a square lattice. The walker starts at the origin. At time $t = 0$, the loop-erased random walk (LERW) is defined to be of length 0, and origin is the only site occupied by the LERW. At every time step, the walker takes one step with equal probability in the four possible directions and the length of the walk increases by one. If the walker reaches a site already occupied by the LERW, the walker has formed a loop. If the loop has ℓ steps, the entire loop is erased, and the length of the (loop-erased) walk decreases by ℓ. The sites in the loop (except the end point) are no longer part of the loop-erased walk.

As the walker continues to walk, at each time step, initially the length of walk increases by one, but the decrease of length occurs whenever loops are formed. At very long times, on a finite lattice of linear size L, there is a stationary state in which the average length of walk is $\mathcal{O}(L^z)$, with $z < 2$. The graph of perimeter of erased loop as a function of time would qualitatively look like Fig. 2. The probability that in the steady state, the size of the erased loop is ℓ varies as an inverse power of ℓ [15].

3.3. Takayasu model of diffusing particles with aggregation

The Takayasu model describes a very different physical phenomena [16]. It describes a system in which particles are continuously injected, diffuse, and coalesce. In its simplest example, it can be defined on a one-dimensional chain. The explicit rules of evolution are:

1. At each time step, each particle in the system moves by a single step, to the left or to the right, taken with equal probability, independent of the choice at other sites.
2. A single particle is added at every site.
3. If there are more than one particles at one any site, they coalesce and become a single particle whose mass is the sum of the masses of the coalescing parts. In all subsequent evolution, the composite particle acts as a single particle.

A quantity of interest in this system is the probability distribution of the total mass at a randomly chosen site at late times. Since mass is added all the time and cannot escape, the average mass per site is proportional to t. It is found that the distribution of mass is a power law, with an upper cutoff that increases with time.

The analogue of avalanches in this model is the event of coming together of large masses. In fact, we will show later that the model is equivalent to a directed version of the sandpile model.

3.4. The train model

Let us define a discrete variation of a model known in literature as the train model [17]. We consider a set of N mass points that are joined to each other by links to form a 'train'. The mass points sit on the sites of a linear chain, the position of the ith mass point being x_i. At time $t = 0$, we start with $x_i = N + 1 - i$.

The links are stretchable, and allowed values of $x_i - x_{i+1}$ are 1 or 2. The first point (the 'engine') moves at a constant rate of one unit at each (discrete-) time step, and it pulls the other mass points behind it with the following rules: If x_i changes to x_i' such that $(x_i' - x_{i+1})$ becomes greater than 2, then x_{i+1} is moved to the right to a new position $x_{i+1}' = x_i' - 1$ or $x_{i+1}' = x_i' - 2$, with equal probabilities $1/2$ each. We update $\{x_i\}$ sequentially from starting with x_1. One update of all masses constitutes one time step.

Clearly, the motion of the engine is deterministic with $x_1(t) = N + t$. However, the other masses undergo a jerky motion, and in particular, the motion of the x_N occurs in bursts, whose size can be very big if N is large. Again, the probability that x_N increases by Δx_N in a single time-step has a power law dependence on Δx_N for large N.

We could continue with many more examples [18]. But perhaps this is enough to give some flavor of the models that have been devised. Admittedly, the models are very simplified, but the analysis of these models is still rather nontrivial.

4. Criticality of the BTW model

It is easy to see that conservation of sand grains in the BTW model implies that on adding a single grain to a stable configuration in the steady state, events involving many topplings must occur with significant probability. Since every particle added anywhere in the system finally leaves the system from the boundary, and on the average it must take at least order L steps to reach the boundary, we see that the average number of topplings per added particle is at least of order L. In other words, we must have for all L

$$\langle s \rangle \equiv \sum s \, \mathsf{Prob}_L(s) \geqslant cL. \tag{2}$$

where c is some constant [19]. If we take the large size limit $L \to \infty$, and define

$$\mathsf{Prob}_\infty(s) = \lim_{L \to \infty} \mathsf{Prob}_L(s). \tag{3}$$

Then, we must have $\int \mathrm{d}s \, s \, \mathsf{Prob}_\infty(s) = \infty$. Such a diverging expectation value can not be generated by any distribution for which the probability of avalanches of size *larger than s* decreases with s faster than $s^{-1-\varepsilon}$, where ε is any positive power. Thus the distribution must be of the type sketched in Fig. 3 with a small enough decay exponent.

This argument suggests that so long as sand can leave the system only at the boundaries, the distribution of avalanches must have a power law tail. In fact, careful experiments with real sand do *not* see such a tail. How to reconcile this with the seemingly robust argument given above?

It seems that the hypothesis of a single angle of repose is not quite correct. There are at least two angles: an angle of stability θ_1, and an angle of drainage θ_2, with θ_1 greater than θ_2 by about a couple of degrees. As we add sand, the slope slowly increases from θ_2 to θ_1, and then there is a single big avalanche and the net slope decreases to θ_2. In such a "charge and fire" behavior, the big avalanches are nearly periodic.

Speaking more mathematically, one can have diverging first moment of a distribution with no power law tail, if the distribution consists of two parts: a small events part which has almost all the weight of the distribution, and a small weight (of order L^{-a}) at a rather large value of $s \sim L^b$. As one needs to build up $O(L^3)$ particles to increase the slope by a finite amount, and in a big event, a particle will move by an amount of order L, this would imply that for a sandpile showing 'charge and fire' behavior, $a = 3, b = 4$. Of course, the existence of large events does not *exclude* a weak power law tail in the small events.

Whether real granular media show SOC or not seems to depend on the shape and friction of grains. The scenario outlined above seems to describe sandpiles with nearly spherical grains. However, if the grains are very rough and of large aspect ratio, they behave differently. In a beautiful series of experiments, Frette et al. have shown that piles formed of long-grain rice do show SOC behavior [20].

The preceding discussion assumed a separation of time scales between the slow driving and relaxation scales, so that an avalanche is finished before the next one starts. It has been argued that infinitesimal driving should be considered as a defining characteristics of SOC [21]. This does not seem to be desirable. We will show later that the Takayasu aggregation model is mathematically equivalent to the sandpile model. But for the Takayasu model, the driving rate is finite. It thus provide an example of a system which displays SOC without the requirement of infinitesimal driving.

We note that so long as there is a wide probability distribution of sizes of events, the interval between rarer events defines a long lime-scale. So the separation of time-scales between the driving scale, and the interval-between-rare-events -scale is automatic. In sandpiles driven at a non-zero rate, one may look for bursts of large activity in a local region of space. Note that if particles are added at a finite rate per site, one needs to also assume a finite probability of loss of particles per toppling in the bulk, if one wants to take the large size limit [22]. For a longer discussion of criticality in sandpiles at non-zero driving rate, see [23].

5. The abelian sandpile model

5.1. Definition

The BTW model has an important abelian property that simplifies its analysis considerably. To bring out this property in its full generality, it is preferable to work in more general setting. To emphasize the abelian property, which lies at the heart of theoretical analysis, I shall use the descriptive name ASM, rather than the historical, more conventional, nomenclature 'the BTW model' in the following [24]. The ASM is defined as follows [25]:

We consider the model defined on a graph with N sites labeled by integers $1, 2, \ldots, N$ (Fig. 4). At each site i, the height of the sandpile is given by a positive integer z_i. At each time step, a site is chosen at random from a given distribution, the probability of site i being chosen being p_i. Its height is increased by 1 from z_i to $z_i + 1$.

We are also given an integer $N \times N$ matrix Δ, and a set of N integers $\{z_{i,c}\}$, $i = 1$ to N. If for any site i, $z_i > z_{i,c}$ then the site is said to be unstable, and it topples. On toppling at site i, all heights z_j are updated according to the rule

$$\text{If } z_i > z_{i,c}, \text{ then } z_j \to z_j - \Delta_{ij}, \text{ for every } j. \tag{4}$$
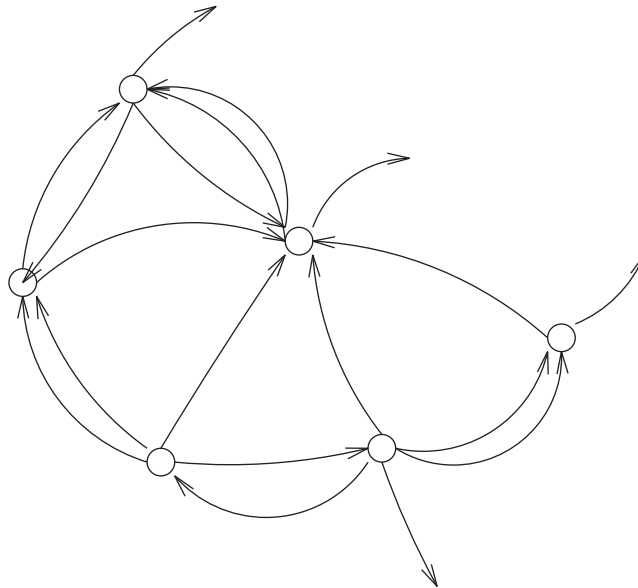

Fig. 4. A graphical representation of a general ASM. Each node denotes a site. The maximum stable height $z_{i,c}$ at the site i equals the number of arrows going out of i. On toppling at any site, one particle is transferred along each bond directed away from the site.

Without loss of generality we may choose $z_{i,c} = \Delta_{ii}$ (this amounts to a particular choice of the origin of the z_i variables). In this case, the allowed values of z_i in a stable configuration are $1, 2, \ldots, \Delta_{ii}$.

Evidently the matrix Δ has to satisfy some conditions to ensure that the model is well behaved.

1. $\Delta_{ii} > 0$, for every i. (otherwise topplings never terminate).
2. For every pair $i \neq j$, $\Delta_{ij} \leqslant 0$. (This condition is required to establish the Abelian property, as will be shown shortly.)
3. $\sum_j \Delta_{ij} \geqslant 0$ for every i. (This condition states that sand is not generated in the toppling process.)
4. There is at least one site i such that $\sum_j \Delta_{ij} > 0$. Such sites are called dissipative sites. In addition, the matrix Δ is such that in the corresponding directed graph, there is a path of directed links from any site to one of the dissipative sites. This condition ensures that all avalanches terminate in a finite time.

5.2. The abelian property

Let $\mathscr{C}$ be a stable configuration, and define the operator a_i such that the stable configuration $\mathscr{C}' = a_i \mathscr{C}$ is the one achieved after addition of sand at site i and relaxing. The mathematical treatment of ASM relies on one simple property it possesses [25]: the order in which the operations of particle addition and site toppling are performed does not matter. Thus the operators a_i commute, i.e.,

$$a_i a_j = a_j a_i \quad \text{for every } i, j. \tag{5}$$

To prove this we start by noting that if we have a configuration with two or more unstable sites, then these sites can be relaxed in any order, and the resulting configuration is independent of the order of toppling. Consider two unstable sites i and j. If we topple at i first, this can only increase the value of z_j (by condition 2), and site j remains unstable. After toppling at j also, the height at any site k, as a result of these two topplings, undergoes a net change of $-\Delta_{ik} - \Delta_{jk}$. Clearly toppling first at j, then at i gives the same result. By a repeated use of this property, any number of unstable sites in a configuration can be relaxed in any order, always giving the same result.

Also, the operation of toppling at an *unstable* site i, commutes with that of adding a particle at some site j, for if the site i is unstable and topples, it will do so also if the addition at site j was performed first. By a repeated use of the property that the individual operations of addition and toppling commute with each other, the abelian property of $\{a_i\}$ follows. A longer, more formal, proof is given in [26].

While this property seems very general, it should be noted that it is not shared by most of the other models of SOC like the forest-fire model [27], or even other sandpile models, such as the critical slope model where the toppling condition at site i depends on the height at other sites, or the Zhang model [28] in which the amount of sand transferred depends on the amount by which the local height exceeds the critical value.

5.3. Operator algebra

The operators $\{a_i\}$ satisfy additional relations. For example, on the square lattice, if one adds 4 particles at a given site, the site is bound to topple once, and a particle is added to each of its nearest neighbors. Thus,

$$a_j^4 = a_{j_1} a_{j_2} a_{j_3} a_{j_4}, \tag{6}$$

where $j_1, \ldots, j_4$ are the nearest neighbors of j (Fig. 5).

In the general case one has instead of (6),

$$a_i^{\Delta_{ii}} = \prod_{j \neq i} a_j^{-\Delta_{ij}}. \tag{7}$$

Using the abelian property, in any product of operators $\{a_i\}$, we can collect together occurrences of the same operator, and using the reduction rules (7), we can reduce the power of a_i to be always less than Δ_{ii}. The $\{a_i\}$
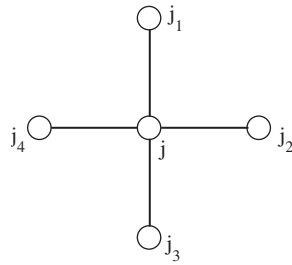
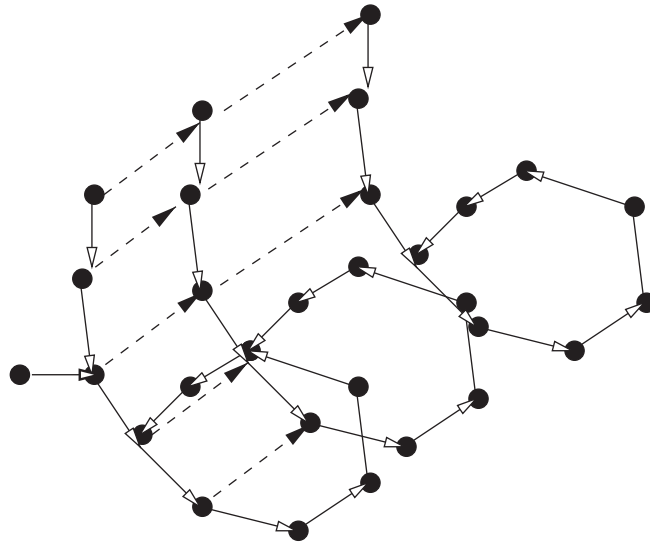Fig. 5. Labelling the neighbors of a site j on the square lattice.

Fig. 6. A schematic representation of action of addition operators on the stable configurations. Each point represents a configuration. Arrows with full lines denote action of the operator a_1. The arrows with dotted lines denote action of the operator a_2.

are therefore the generators of a finite abelian semi-group (the associative property follows from the definition), subject to the relations (7). These relations define the semi-group completely.

Let us consider the repeated action of some generator a_1 on some configuration $\mathscr{C}$. Since the number of possible states is finite, the orbit of a_1 must at some stage close on itself, so that $a_1^{n+p}\mathscr{C} = a_1^n\mathscr{C}$ for some positive period p, and non-negative integer n. The first configuration that occurs twice in the orbit of a_1 is not necessarily $\mathscr{C}$, so that the orbit consists of a sequence of transient configurations followed be a cycle (see Fig. 6). If this orbit does not exhaust all configurations, we can take a configuration outside this orbit, and repeat the process. Thus the space of configurations is broken up into disconnected parts, each containing one limit cycle.

Under the action of a_1 the transient configurations are unattainable once the system has reached one of the periodic configurations. In principle these states might still be reachable as a result of the action of some other operator, e.g. a_2. However, the abelian property implies that if $\mathscr{C}$ is a configuration which is part of one of the limit cycles of a_1, then so is $a_2\mathscr{C}$, since $a_1^p\mathscr{C} = \mathscr{C}$ implies that $a_1^p a_2\mathscr{C} = a_2 a_1^p\mathscr{C} = a_2\mathscr{C}$. Thus, the transient configurations with respect to a_1 are also transient with respect to other operators $a_2, a_3, \ldots$, and hence occur with zero probability in the steady state of the system. The abelian property thus implies that a_2 maps cycles of a_1 to cycles of a_1, and moreover, that all these cycles have the same period (Fig. 6).

We can now repeat our previous argument, to show that the action of a_2 on a cycle is finally closed on itself to yield a torus, possibly with some transient cycles, which may be also discarded. Repeating this argument for the other cycles, and other generators leads to the conclusion that the set of all recurrent configurations forms a set of multi-dimensional tori under the action of the a's.

5.4. The abelian group

If we restrict ourselves to the set **R** of recurrent states, we can define inverse operators a_i^{-1}, for all i as each configuration in a cycle has exactly one incoming arrow corresponding to operator a_i. Thus the a operators generate a group. The action of the a's on the states corresponds to translations on the torus. From the symmetry of the torus under translations, it is clear that all recurrent states appear in the stationary state with equal probability.

This analysis, which is valid for every finite abelian group, leaves open the possibility that some configurations are not reachable from each other, in which case there might be several different mutually disconnected tori. However, such a situation cannot happen in the ASM if we allow addition of sand at all sites with nonzero probabilities (all $p_i > 0$). Then, the configuration $\mathscr{C}_{\max}$, in which all the sites have their maximal height is reachable from every configuration, and is therefore recurrent, and since inverses of a's exist for configurations in **R**, every recurrent configuration is reachable from $\mathscr{C}_{\max}$, implying that all recurrent states lie on the same torus.

If some of the addition probabilities p_i are zero, one has to consider the subgroup formed taking various powers of those a_j's which have nonzero p_j. This may still generate the full group. (On a square lattice of size $L \times L$, the number of independent generators of the group can be shown to be only L [29], and hence if one selects $L' > L$ generators at random, with a large probability one generates the full group.) If not, the dynamics splits **R** to several disconnected tori, and the steady state is non-unique. It does not fully forget the initial condition, as the evolution is confined to the torus on which it started. We will discuss an example of this type later, in Section 8.

5.5. The evolution operator and the steady state

We consider a vector space $\mathscr{V}$ whose basis vectors $|\mathscr{C}\rangle$ are labelled by the different configurations of **R**. The state of the system at time t will be given by a vector $|P(t)\rangle \in \mathscr{V}$

$$|P(t)\rangle = \sum_{\mathscr{C}} \mathsf{Prob}(\mathscr{C}, t)|\mathscr{C}\rangle, \tag{8}$$

where $\mathsf{Prob}(\mathscr{C}, t)$ is the probability that the system is in configuration $\mathscr{C}$ at time t. The operators a_i can be defined to act on the vector space $\mathscr{V}$ through their operation on the basis vectors.

The time evolution is Markovian, and governed by the equation

$$|P(t+1)\rangle = \mathscr{W}|P(t)\rangle, \tag{9}$$

where

$$\mathscr{W} = \sum_{i=1}^{N} p_i a_i. \tag{10}$$

To solve the time evolution in general, we have to diagonalize the evolution operator $\mathscr{W}$. Being mutually commuting, the a_i may be simultaneously diagonalized, and this also diagonalizes $\mathscr{W}$. Let $|\{\phi\}\rangle$ be the simultaneous eigenvector of $\{a_i\}$, with eigenvalues $\{e^{i\phi_i}\}$, for $i = 1, \ldots, N$. Then

$$a_i|\{\phi\}\rangle = e^{i\phi_i}|\{\phi\}\rangle \quad \text{for } i = 1 \text{ to } N. \tag{11}$$

Since the a operators now form a group, relations (7) may be written as

$$\prod_j a_j^{\Delta_{kj}} = 1, \quad \text{for every } k. \tag{12}$$

Applying the LHS to the eigenvector $|\{\phi\}\rangle$ gives $\exp(i\sum_j \Delta_{kj}\phi_j) = 1$, for every k, so that $\sum_j \Delta_{kj}\phi_j = 2\pi m_k$, or inverting,

$$\phi_j = 2\pi \sum_k [\Delta^{-1}]_{jk} m_k, \tag{13}$$

where Δ^{-1} is the inverse of Δ, and the m_k's are arbitrary integers.

The particular eigenstate $|\{0\}\rangle$ ($\phi_j = 0$ for all j) is invariant under the action of all the a's, $a_i|\{0\}\rangle = |\{0\}\rangle$. Thus $|\{0\}\rangle$ must be the stationary state of the system since

$$\sum_i p_i a_i |\{0\}\rangle = \sum_i p_i |\{0\}\rangle = |\{0\}\rangle. \tag{14}$$

We can now see explicitly that the steady state is independent of the values of the p_i's and that *in the steady state, all recurrent configurations occur with equal probability*. As discussed above, when some of the p_i's are zero, the stationary state may not be unique. In this case, the general steady state is a linear combination of the eigenvectors of $\mathscr{W}$ having eigenvalue 1.

5.6. Algebraic structure of the abelian group

Any finite abelian group Z can always be expressed as a product of cyclic groups in the following form:

$$Z \cong \mathbf{Z}_{d_1} \times \cdots \times \mathbf{Z}_{d_g}. \tag{15}$$

That is, the group Z is isomorphic to the direct product of g cyclic groups of orders $d_1, \ldots, d_g$. Furthermore the integers $d_1 \geqslant d_2 \geqslant \cdots d_g > 1$, can be chosen such that d_i is an integer multiple of d_{i+1}, and under this condition, the decomposition is unique. For example, $\mathbf{Z}_6 \times \mathbf{Z}_4 \cong \mathbf{Z}_{12} \times \mathbf{Z}_2$ but $\mathbf{Z}_2 \times \mathbf{Z}_2 \not\cong \mathbf{Z}_4$.

To construct this factorization for the abelian group G for the ASM, we use the following classical result, known as the Smith decomposition [30]: Given an integer $N \times N$ matrix Δ, there exist unimodular integer $N \times N$ matrices A and B, and an integer diagonal matrix D such that

$$\Delta = ADB. \tag{16}$$

[A matrix is said to be unimodular if its determinant is ± 1. The inverse of an integer unimodular matrix is also an integer matrix.] The matrix D is unique if we further impose the condition that its diagonal elements $d_1, \ldots, d_N$ are such that d_i is a multiple of d_{i+1}. The matrices A and B are not unique.

The Smith decomposition is constructed step by step as follows: We define two matrices Δ and Δ' to be similar [to be denoted by $\Delta \sim \Delta'$] if there exist unimodular matrices S_1 and S_2 such that $\Delta = S_1 \Delta' S_2$. Among the unimodular matrices there are matrices P_{ij} which interchange the rows i and j acting on the left and columns i and j acting on the right, as well as $Q_{ij}(n)$ which add n times row (column) j to row (column) i acting on the left (right). Explicitly, P_{ij} is just the identity with rows i and j interchanged, and $Q_{ij}(n)$ is the identity with an additional n in the (ij)th position.

Let Δ_{ij} be one of the non-zero elements of Δ having the smallest absolute value. Operating with interchange matrices, we can get an equivalent matrix Δ' in which this element m occurs in the lower right corner. Then, by multiplication with the matrices of type Q, all the other members of the last row and last column are replaced by their remainders modulo m. If any of the remainders are non-zero, the smallest one may be shifted to the corner, and the process repeated until the last row and column are zero except for the corner element:

$$\Delta \sim \begin{pmatrix} \Delta^{(1)} & \begin{matrix} & & 0 \\ & & \vdots \end{matrix} \\ 0 \cdots & d_N \end{pmatrix}. \tag{17}$$

Then, if any of the still nonzero elements of the resulting matrix is not divisible by the element d_N in the lower right corner, its row may be added to the last row, and as before the remainder is brought to the corner. Thus, d_N can be chosen to be the greatest common divisor of all the elements of the original matrix Δ.

Applying the same process reduces $\Delta^{(1)}$ to matrix $\Delta^{(2)}$ which has additionally row and column $N - 1$ empty except for the $(N - 1, N - 1)$th element which is the gcd of the elements of $\Delta^{(1)}$ except d_N. This procedure finally yields the matrix D and the products of P and Q matrices used give the matrices A and B.

Given the Smith decomposition of Δ, we can define generators of the cyclic subgroups of the group G by

$$e_\alpha = \prod_j a_j^{B_{\alpha j}}, \quad \alpha = 1, \ldots, g. \tag{18}$$

It is then easy to see that

$$e_\alpha^{d_\alpha} = \prod_j a_j^{[DB]_{\alpha j}} = \prod_j a_j^{[A^{-1}\Delta]_{\alpha j}} = 1, \quad \alpha = 1,\ldots,g, \tag{19}$$

where we have used Eq. (12).

For any configuration $\{z_i\}$, we define scalar functions I_α, for $\alpha = 1\ldots g$, linear in the height variables by the equations

$$I_\alpha = \sum_{j=1}^{N} z_j [B^{-1}]_{j\alpha}. \tag{20}$$

As a result of toppling at k, the change in z_j is by an amount $-\Delta_{kj}$, so that the change in I_α, denoted by δI_α, is

$$\delta I_\alpha = -\sum_j \Delta_{kj}[B^{-1}]_{j\alpha} = -[\Delta B^{-1}]_{k\alpha} = -[AD]_{k\alpha} = -A_{k\alpha}d_\alpha, \tag{21}$$

which shows that $I_\alpha \bmod d_\alpha$ is invariant under toppling. Thus, it follows that with each equivalence class is associated a single set of integers $[I_1,\ldots,I_g]$, where I_α is defined modulo d_α.

The action of the operators e_α on the I's is such that

$$I_\beta(e_\alpha\{z\}) - I_\beta(\{z\}) = \sum_j B_{\alpha j}[B^{-1}]_{j\beta} = \delta_{\alpha\beta}, \tag{22}$$

which means that the e_α's are the generators of the cyclic subgroups in the decomposition (15), and that the I_α's can serve as coordinates along the respective cycles.

Eq. (22) also implies that each of the possible values of $[I_1,\ldots,I_g]$ is reachable. Since the number of such configurations is $\prod_{\alpha=1}^{g} d_\alpha = \det \Delta$, we conclude that each recurrent configuration may be uniquely labeled by the $\{I\}$ variables.

Calculation of properties in the steady state involves an average over all recurrent states. Using the height variables to characterize configurations is not very convenient here, because the existence of FSC's (defined in the next section) implies many nontrivial constraints in the values of $\{z_i\}$ used in the sum. The summations over I_α are independent of each other, hence formally simpler. The explicit calculation of the matrices A and B is however nontrivial; and has not been done in any nontrivial case.

The toppling invariants $\{I\}$ are very useful in another way. Consider a general toppling invariant I which is linear in the height variables $\{z_i\}$, of the form

$$I_\alpha = \sum_{i=1}^{N} g_{i\alpha}z_i \pmod{d_\alpha}, \tag{23}$$

where $g_{i\alpha}$ are some integer constants. The values of the constants depends on Δ. We define unitary operators S_α corresponding the toppling invariant I_α by the equation

$$S_\alpha = \exp(2\pi i I_\alpha/d_\alpha), \quad \alpha = 1,\ldots g. \tag{24}$$

These operators are diagonal operators in the configuration basis. It is easy to see that their commutation with $\{a_i\}$ are given by the equation

$$S_\alpha a_i S_\alpha^{-1} = \exp(2\pi i g_{i\alpha}/d_\alpha)a_i. \tag{25}$$

This implies that if $|\psi\rangle$ is a simultaneous right eigenvector of the operators $\{a_i\}$ with eigenvalues $\{a_i\}$, then $S|\psi\rangle$ is also a right eigenvector of these operators with a different set of eigenvalues $\exp(2\pi i g_{i\alpha}/d_\alpha)a_i$. Thus S_α act as ladder operators also for the evolution operator $\mathcal{W}$.

5.7. Propagation of avalanches: the two-point function

An important quantity characterizing the steady state is its response to a small perturbation. Here it can be measured by the probability that a single particle added at some site causes a perturbation which affects a site at a distance R from it. Let G_{ij} be the expected number of toppling at site j, upon adding a particle at site i *in the steady state*. Since in the steady state the expectation value of the number of particles at a site is constant, there must exist a balance between the average influx of particles from toppling at other sites, and the outflux from toppling at the site. For the square lattice model, this relation gives (Fig. 5)

$$G_{ij_1} + G_{ij_2} + G_{ij_3} + G_{ij_4} = 4G_{ij}, \tag{26}$$

where $i \neq j$. In the general case we have

$$\sum_k G_{ik} \Delta_{kj} = \delta_{ij}, \tag{27}$$

where the δ_{ij} takes account of the addition of one particle at i. Solving for G gives simply

$$G_{ik} = [\Delta^{-1}]_{ik}. \tag{28}$$

Note that this derivation does not use the abelian property, only the fact that the mass transferred in each toppling is the same. It is therefore valid for a much wider class of models. Such an equation still holds if the toppling condition is a critical slope condition, but not if the number of particles transferred depends on the slope.

In the case of a d-dimensional hypercubical lattice, with particle transfer to nearest neighbors, and loss of sand only at the boundary, this is just the inverse of the lattice Laplacian. Then it is easy to see that

$$G_{ik} \sim r_{ik}^{2-d} \quad \text{for } d > 2; \tag{29}$$
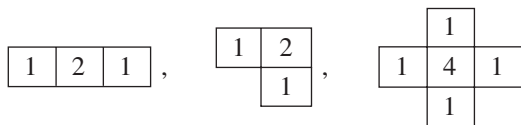$$\sim \log(L/r_{ik}) \quad \text{for } d = 2; \tag{30}$$
$$\sim (L - r_{ik}) \quad \text{for } d = 1, \tag{31}$$

where L is the size of the lattice. We note that the influence function G does show the promised long-ranged correlations.

6. Recurrent and transient configurations

Given a stable configuration of the pile, how can we tell if it is recurrent or transient? A first observation is that there are some forbidden subconfigurations which can never be created by addition of sand and relaxation, if not already present in the initial state. The simplest example on the square lattice case is a subconfiguration of two adjacent sites of height 1, $\boxed{1}\boxed{1}$. Since $z_i > 0$, a site of height 1 may only be created as a result of a toppling at one of the two sites (toppling anywhere else can only add particles to this pair of sites). But a toppling of either of these sites results in a height of at least 2 at the other. Thus, any configuration which contains two adjacent 1's is transient. The argument may now be repeated to prove that subconfigurations such as

$$\boxed{1}\,\boxed{2}\,\boxed{1} \,, \qquad \begin{array}{cc} \boxed{1} & \boxed{2} \\ & \boxed{1} \end{array} \,, \qquad \begin{array}{ccc} & \boxed{1} & \\ \boxed{1} & \boxed{4} & \boxed{1} \\ & \boxed{1} & \end{array}$$

also can never appear in a recurrent configuration.

In general, a forbidden subconfiguration (FSC) is a set of connected sites F such that the height z_j of each site j in F, is less than or equal to the number of neighbors of j in F. The proof of this assertion is by induction on the number of sites in F. For example, creation of the $\boxed{1}\boxed{2}\boxed{1}$ configuration, must involve toppling at one of the end sites, but then the configuration must have had a $\boxed{1}\boxed{1}$ before the toppling. But this was shown before to be forbidden, etc.

6.1. The 'multiplication by identity' test

A more systematic way to test for recurrence of a given configuration is by using the relations (7). Let us take up again the example of the sandpile defined on an $L \times M$ square lattice. Multiplying all the relations gives

$$\prod_i a_i^4 = \prod_i a_i^{n_i}, \tag{32}$$

where n_i is the number of neighbors of a given site, i.e., 4 for a bulk site, 3 or 2 for a boundary site. Now we use the property that inverses are defined on the set **R** of recurrent states, which allows cancellation, yielding

$$\prod_i a_i^{4-n_i} = 1. \tag{33}$$

In other words, in order to check whether a given configuration $\mathscr{C}$ is recurrent, one has to add a particle at each boundary site (2 at corners), relax the system, and check whether the final configuration is same as $\mathscr{C}$. If it is, $\mathscr{C}$ is recurrent, otherwise it is not [31].

An interesting consequence of the existence of forbidden configurations is the following: Consider an ASM on an undirected graph with N_s sites and N_b bonds between sites. Then in any recurrent configuration the number of sand grains is greater than or equal to $N_s + N_b$. Note that here we do not count the boundary bonds that correspond to particles leaving the system. To prove this, we just observe that if the inequality is not true for any configuration, it must have an FSC in it (proof by induction on N_s).

6.2. The burning test

As explained above, a recurrent configuration is characterized by being invariant under addition of particles at the boundary in a judicious fashion, and relaxing. When the matrix Δ is symmetric, this test is equivalent to a simpler test, called the burning test, which is defined as follows [32]: given a configuration, at first all the sites are considered unburnt. Then, burn each site whose height is larger than the number of its unburnt neighbors. This process is repeated recursively, until no further sites can be burnt. Then, if all the sites have been burnt, the original configuration was recurrent, whereas if some sites remain unburnt, then the original configuration was transient, and the remaining sites form an FSC.

As an example, let us take a configuration on a 4×4 square lattice shown below. Its evolution under burning is as shown:
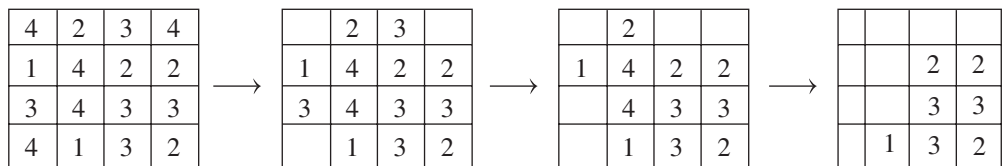
where burned sites are denoted by empty squares. At first the 'fire' burns some of the boundary sites, and it then advances inward. No site in the last configuration can be burned, and the set of unburnt sites is thus a forbidden subconfiguration. If the height of the third site on the second row were changed from 2 to 3, then it could be burned next, and the fire would have spread completely, and such a configuration would be recurrent.

It is obvious that the burning process is in fact identical to toppling, starting from addition at the boundary, except that it is simpler to use, as we work with initial height configuration, and do not need to keep updating them with each toppling, since we know that the final configuration is the same as the starting one, if all sites topple exactly once.

To see what could go wrong when Δ is asymmetric consider the example of a two site sandpile with a toppling matrix $\begin{pmatrix} 7 & -2 \\ -4 & 2 \end{pmatrix}$. In the unsymmetrical case, a site is burnt if its height exceeds the number of outgoing bonds to unburnt neighbors. A configuration with five grains at 1, and one grain at 2 would pass the burning test, but is in fact transient. A site like site 2, which has more incoming arrows than outgoing arrows is called a greedy site. In this case, equations satisfied by the operators a_1 and a_2 are $a_1^7 = a_2^4$, and $a_2^2 = a_1^2$. This gives the

identity operator as $a_1^3 = 1$, but adding three particles on site 1 in a recurrent configuration, we get one toppling at site 1, but two topplings at site 2. Clearly, the burning test fails as it assumes that under multiplication by the identity operator [Eq. (11)], each site topples only once. We also see that if there are no greedy sites, the burning test is a necessary and sufficient test for recurrence even for unsymmetrical graphs.

6.3. Number of recurrent configurations

What is the total number of recurrent configurations? If we were to take care of only the constraint that $\boxed{1\ 1}$ is disallowed, this problem becomes the nearest-neighbor exclusion lattice gas model for a particular value of fugacity of particles, which is a special case of the famous unsolved problem of the Ising model in a magnetic field. However, it turns out the infinity of the FSC constraints actually can be taken care of, and the final result is rather simple: the total number of recurrent configurations $|\mathbf{R}|$ is given by

$$|\mathbf{R}| = \det \varDelta. \tag{34}$$

Consider the set of all possible configurations $\{z_i\}$, $-\infty < z_i < \infty$. We can define an equivalence relation on this set of configurations as follows: We call two configurations $\mathscr{C}$ and $\mathscr{C}'$ as equivalent if one can be obtained from the other by a series of topplings and untopplings [untoppling is the reverse of toppling, in an 'untoppling' at site i, the height at all sites j is *increased* by an amount $\varDelta_{ij}$]. For this purpose, we can topple or untopple at any site whatever be its local height at that time. This is equivalent to defining $\mathscr{C} \sim \mathscr{C}'$ if and only if

$$z_j = z_j' - \sum_i m_i \varDelta_{ij} \tag{35}$$

for some integers $\{m_i\}$, $i = 1, \ldots, N$. The members of an equivalence class form a superlattice of $\mathbf{Z}^N$, with the rows of $\varDelta$ as basis vectors (Fig. 7). It is easily shown that each equivalence class contains exactly one recurrent configuration.

Firstly, starting with any configuration, if we untopple once at all sites, we get an equivalent configuration with an increased number of sand grains in the system. We then relax the resulting configuration. As this process, equivalent to adding particles and relaxing, can be repeated, the stable configuration thus reached is recurrent. Thus, each equivalence class has at least one recurrent configuration.
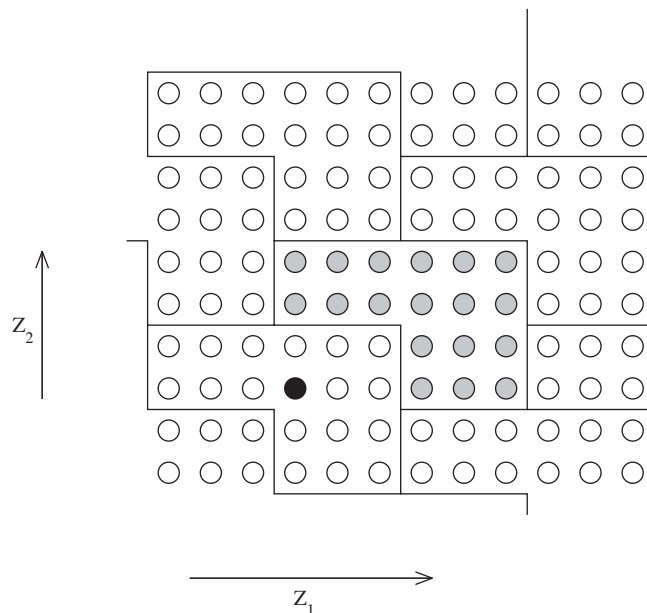

Fig. 7. The superlattice of equivalent configurations in the space of all configurations (z_1, z_2) for a 2-site automata with $\varDelta = \begin{bmatrix} 6 & -2 \\ -3 & 4 \end{bmatrix}$ with copies of the recurrent set $\mathscr{R}$. The gray vertices are the recurrent configurations. The black circle marks the configuration $(1, 1)$.

Now, we argue that there can be at most one recurrent configuration in each equivalence class. Assume the contrary. Let $\{z_i\}$ and $\{z'_i\}$ be two equivalent stable configurations. Let m_{max} be the maximum value of m_i in Eq. (35) over all i, and F be the set of sites for which this maximum value is reached. Then, to go from $\{z'_i\}$ to $\{z_i\}$, each site in F topples at least one more time than its neighbors outside F. Hence each site in F would lose one particle to each neighbor outside F in going from $\{z'_i\}$ to $\{z_i\}$. If $\{z'_i\}$ is stable, this implies that F must be an FSC in $\{z_i\}$. This implies that $\{z_i\}$ is not recurrent, which contradicts the assumption. Therefore, the number of elements of **R** must be equal to the volume of the unit cell of the superlattice. But this is clearly det Δ. This proves Eq. (34).

7. Potts model, spanning trees, resistor networks, and loop-erased random walks

In this section, we shall use the burning test to relate the undirected ASM to a well-known model of classical statistical mechanics: the Potts model. The generating function for the number of recurrent configurations with a given number of grains can be expressed in terms of the partition function of the Potts model in a particular limit. This relationship also allows one to relate the ASM problem to other well-studied problems in lattice statistics and graph theory: the spanning trees problem, the resistor networks, and the loop-erased random walk.

7.1. The Potts model

The q-state Potts model is defined on a graph G, with 'spin' variables σ_i defined at its nodes taking q discrete values, which may be labelled by integers between 1 and q. The Hamiltonian is

$$H[\{\sigma\}] = -\sum_{i<j} J_{ij}\delta(\sigma_i, \sigma_j), \tag{36}$$

where the sum is over the nodes of the graph. The coupling J_{ij} is nonzero if and only if nodes i and j are linked. This is a generalization of the well-known Ising model which corresponds to the special case $q = 2$. We write

$$\exp[J_{ij}\delta(\sigma_i, \sigma_j)] = [1 + v_{ij}\delta(\sigma_i, \sigma_j)], \tag{37}$$

where $v_{ij} = \exp(J_{ij}/T) - 1$. The partition function of the Potts model can then be written as

$$Z(q, T) = \sum_{\{\sigma\}} \prod_{E(G)} [1 + v_{ij}\delta(\sigma_i, \sigma_j)], \tag{38}$$

where the product is over the set of edges $E(G)$ and the summation takes each spin variable over its q possible values.

We expand the right-hand side as a sum of products of the v's. Each term of this sum can be represented as a graph, in which we represent the term v_{ij} by the edge (ij) being occupied, and 1 by the edge remaining unoccupied. The different terms of the expansion correspond to all possible (2^E, where E is the total number of nonzero J_{ij}'s) configurations of occupied and unoccupied edges of the graph. For any one such configuration of edges, the sum over $\{\sigma_i\}$ can now be done explicitly, and we get $q^{c(\mathbf{E}')}$ where $c(\mathbf{E}')$ is the number of disconnected clusters in the configuration of edges $\mathbf{E}'$.

Thus expression (38) can be rewritten in the form, as was done first by Fortuin and Kasteleyn [33], as sum over the subsets $\mathbf{E}'$ of the set of edges $\mathbf{E}$

$$Z(q, T) = \sum_{\mathbf{E}' \subset \mathbf{E}} q^{c(\mathbf{E}')} v^{\mathbf{E}'}, \tag{39}$$

where $v^{\mathbf{E}'}$ is the product of the weights v_{ij} over all the edges in $\mathbf{E}'$. Being a polynomial in q, Eq. (39) may be used to define the partition function of the Potts model for an arbitrary non-integer value of q.

7.2. Relation between the Potts model and the ASM

In order to relate the undirected ASM to the spanning trees problem, we consider the graph obtained by adding a sink site to the (undirected) graph specifying the ASM, and connect the sink site to all the boundary sites (called dissipative sites previously) by as many bonds as the number of sand grains dissipated at that site.

We calculate the Potts model partition function on this augmented graph $\mathscr{G}^*$ in the limit $q \to 0^+$. In this limit, only the terms in $Z(q, T)$ with $c(\mathbf{E}') = 1$ contribute. We put bond-weights $v_{ij} = v$ for all edges present in the graph. This graph has $N + 1$ sites (including the sink site), and if all sites belong to a single cluster $\mathbf{E}'$ must have at least N bonds. Hence we get

$$Z(q \to 0^+, T) = qv^N H(v) + \text{terms of order } q^2, \tag{40}$$

where $H(v)$ is a polynomial in v of maximum degree $E - N$. (Here E is the total number of edges in $\mathbf{E}$.)

The connection between the ASM and the Potts model comes from the following result [34]: let $\mathscr{C}$ be any recurrent configuration of the ASM. We define the total mass of $\mathscr{C}$, $m(\mathscr{C})$, as the total number of grains in the configuration $\mathscr{C}$. Let $\mathscr{N}_m$ be the number of recurrent configurations having mass m. The generating function $\mathscr{N}(y)$ is defined by the equation

$$\mathscr{N}(y) = \sum_m \mathscr{N}_m y^m. \tag{41}$$

It is easy to see that the minimum value of m is $N + E - E_s$, where E_s is the number of edges coming to the sink site, and the maximum value is $2E - E_s$ [Proof by induction on the number of edges in the graph]. Then we have

$$\mathscr{N}(y) = y^{N+E-E_s} H(v = y - 1). \tag{42}$$

To establish this result, we regroup terms of the summation in Eq. (39) and associate a recurrent configuration of the ASM with each group. This is done using the burning test.

In the test as defined in Section 4.2, the order in which sites are burnt is unimportant, and the final outcome is independent of the order in which sites are burnt. For our present purpose, it is convenient to use a parallel updating procedure. The fire starts at the sink site at time $t = 0$. At time $t = 1$, all burnable sites connected to the sink are burnt. This renders some more sites burnable. These are burnt at time $t = 2$, and so on. In this way, we can define a 'burning time' for each site in a recurrent configuration.

For each edge-set $\mathbf{E}'$ in Eq. (39), we associate a recurrent configuration $\mathscr{C}$ of the ASM such that for each site i in G, its burning time in the $\mathscr{C}$ is equal to the minimum number of steps needed to reach it from the sink site, using only the edges in $\mathbf{E}'$.

Given $\mathbf{E}'$, it is straight-forward to construct the set of burning-times of different sites in the corresponding configuration $\mathscr{C}$. From the set of burning times, we now try to construct the heights $\{z_i\}$. The set of burning times $\{t_i\}$ does not determine the heights uniquely. To assign $\mathscr{C}$ uniquely to each $\mathbf{E}'$, we need additional rules.

To start with, we note that if a site i has burning time t_i, it must have at least one site with a burning time $t_i - 1$. If it has r_i nearest neighbors with burning time $t_i - 1$, and s_i neighbors with burning time *less than or equal to t*, then its height z_i must satisfy $s_i + 1 \leqslant z_i \leqslant s_i + r_i$ (else it would have burnt earlier).

To fix z_i, when r_i is greater than 1, we choose the following convention: We order all the edges incident at i in some way. This ordering can be chosen independently at each site i, but once chosen remains the same for all $\mathbf{E}'$. Now, we arrange the r_i edges connecting i to its neighbors with burning time $t_i - 1$, using this order relation. Say the edges are $e_1 > e_2 > \cdots > e_{r_i}$. We examine the edges one after another, until we find the first edge that is present in $\mathbf{E}'$. If it is the uth entry in the list, we choose to assign this to configuration with $z_i = s_i + r_i + 1 - u$.

Clearly, with this rule, different $\mathbf{E}'$ get mapped to same configuration $\mathscr{C}$. In fact, once an edge e_u is present in $\mathbf{E}'$, whether the subsequent edges in the list are present in $\mathbf{E}'$ or not makes no difference. Also, the total number of such unexamined edges is clearly equal to the excess height in the configuration $\mathscr{C}$. For example, if we have a minimal sandpile configuration which lowest allowed heights consistent with a given set of burning times, it would have no unexamined edges. If there are n unexamined edges, summing over all configurations of these, gives a factor $(1 + v)^n$. There are exactly N edges that were examined and found present (one per site). Thus,
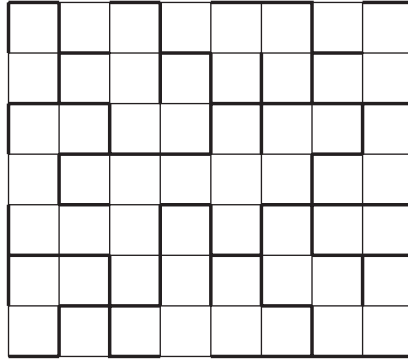
Fig. 8. A spanning tree (marked by thick lines) on a 9×8 square lattice.

we see that Eq. (40) can be written as

$$Z(q \to 0^+, T) = qv^N \sum_{\mathscr{C}} (1 + v)^{m(\mathscr{C}) - m_0}, \tag{43}$$

where m_0 is the minimum mass of a recurrent configuration. This then immediately gives us Eq. (42).

This, in principle, gives us full information about the relative number of configurations of different total mass in the recurrent states. Unfortunately, explicit evaluation of this partition function is not easy. It has been calculated so far only for simple cases like the linear chain, and the Bethe lattice.

7.3. Relation to spanning trees

If we take the double limit $q \to 0^+$ and small v, i.e., in the high-temperature limit, we put $v_{ij} = \beta w_{ij}$, and let β tend to zero. Then, this picks out one component subgraphs with a minimal number of edges, which are just the spanning trees (Fig. 8). In summary, we have the following:

$$\lim_{\beta \to 0} \beta^{-N+1} \lim_{q \to 0} q^{-1} Z(q, T) = \mathscr{T}(G). \tag{44}$$

Here $\mathscr{T}(G)$ is the sum of weights of all the spanning trees on the graph G. This equals the number of spanning trees on the same graph, if we put $w_{ij} = 1$ if an edge (ij) is present in G, and $w_{ij} = 0$ otherwise. The equivalence to the Potts model is very useful, as a large number of results are known for the Potts model. An overview of these may be found in the review by Wu [35].

In two dimensions, the conformal invariance of the critical state restricts strongly the possible critical exponents, and in fact the critical exponents of the Potts model in two dimensions are known for all q. For $q \to 0$ Potts model, the corresponding field theory has central charge $c = -2$ [36]. In this case, most of the exponents are simple (for example, we have already seen that the 2-point correlation function is just the inverse Laplacian). There is one non-trivial exponent which refers to the fractal dimension of chemical paths in the spanning tree representation. If two points are separated by a Euclidean distance r, the conformal field theory predicts that the average length of the path along the tree varies as $r^{5/4}$. Since the spanning tree describes the propagation of 'fire' (i.e., activity) in the system, the chemical path measures the time taken for the activity to travel to distance r. Thus, we conclude that average time for avalanche to spread to distance r varies as $r^{5/4}$ in two dimensions.

In the previous construction, if we delete all the unexamined edges from $\mathbf{E}'$, we are left with exactly N edges that form a single loopless cluster on the graph $\mathscr{G}^*$ having $N + 1$ vertices, i.e., it is a spanning tree (see Fig. 8). Our procedure then, gives a one-to-one correspondence between the recurrent configurations of ASM and spanning trees on the corresponding augmented graph.

There is a symmetric matrix associated with each such undirected graph, called the adjacency matrix of the graph. Let us denote it by M. It is defined such that the off-diagonal element M_{ij} is the negative of the number of
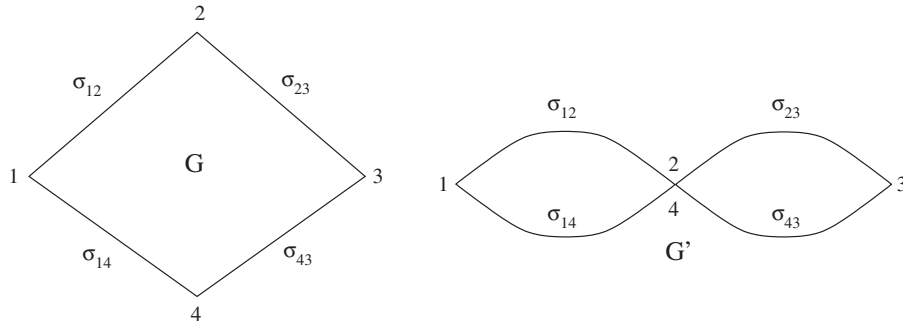
Fig. 9. An example of the Kirchoff formula for resistor networks. The conductances of individual links are shown in the network graph G. Identifying the sites 2 and 4 we get the graph G'. In this case, $T(G) = \sigma_{12}\sigma_{23}\sigma_{14}\sigma_{43}(\sigma_{12}^{-1} + \sigma_{23}^{-1} + \sigma_{14}^{-1} + \sigma_{43}^{-1})$ and $T(G') = (\sigma_{12} + \sigma_{14})(\sigma_{23} + \sigma_{43})$. Here $R_{24} = T(G')/T(G)$.

links between nodes i and j, and M_{ii} equals the number of links attached to node i. The well-known matrix-tree theorem in graph theory [37] states that the number of different spanning trees one can construct on the graph is equal to the determinant of a matrix obtained by deleting an arbitrary column and an arbitrary row from M.

If one constructs the matrix M associated with the graph of the ASM, deleting the row and column of the sink site, one recovers the toppling matrix Δ. By the matrix tree theorem, the number of spanning trees on the graph is det Δ, and by the one-to-one correspondence, this is also the number of recurrent configurations, as we have already seen.

7.4. Relation to the resistor network model

The connection of spanning trees makes the ASM problem equivalent to another classical problem in lattice statistics: the resistor network problem. We are given a set of resistors with different conductances connected to each other in some way. Suppose there are N nodes with a resistor with conductance σ_{ij} between the nodes i and j. [If there is no resistor between i and j, we set $\sigma_{ij} = 0$]. The problem is to find the equivalent resistance between any two given nodes of the network.

This problem is usually solved by setting up N linear equations between the voltages at nodes (the Kirchoff equations), and solving them. We only note here the final result: Represent the network as a graph G with the link between node i and node j having the weight σ_{ij}. We construct spanning trees on this graph, and define the weight of a tree as the product of σ's of the occupied links. We define $T(G)$ as the sum of weights of all spanning trees on the graph G. Clearly $T(G)$ is a homogeneous polynomial of σ_{ij}'s of degree $N - 1$. Then

$$R_{ij} = T(G')/T(G), \tag{45}$$

where R_{ij} is the effective resistance between the nodes i and j, and G' is a graph obtained from G by identifying the nodes i and j [35]. As a simple check, one can verify that for simple series and parallel connection of resistors, this formula gives the right answer (Fig. 9). That R_{ij} is expressible as a ratio of two determinants may have been expected, as it is a solution to a linear set of equations. In the Kirchoff formula [Eq. (45)], each of the determinants is expressed as a sum over weighs over all spanning trees of certain graphs.

The two-point correlation function G_{ij} has a simple interpretation in the language of resistor networks. We consider a resistor network corresponding to the graph of the ASM, where each bond is a unit resistor. The sink site is always kept at potential 0 by definition. Then, the two-point correlation function G_{ij} satisfies Eq. (27), and can be interpreted as the potential produced at node j when a unit current fed in at i, and the current is taken out from the sink node.

7.5. Waves of toppling

We have already seen that topplings in an ASM can be done in any order. One very useful way to relax is by a succession of waves of topplings. Let the site where new grain is added be O. If after addition, O is still

stable, the relaxation process is over. If it is unstable, we relax it as follows: topple O once, and then allow the avalanche to proceed by relaxing any unstable sites, without however toppling O again. This constitutes the first wave of toppling. If at the end, site O is still unstable, we allow it to topple once more, and let the other sites relax, until all sites other than O are stable. This is the second wave of toppling. Repeat as needed. Eventually, site O is no longer unstable at the end of a wave, and the relaxation process stops. It is easy to see that in any wave, the set of toppled sites forms a connected cluster with no voids (untoppled sites fully surrounded by toppled sites), and no site topples more than once in one wave. (This would not be true if the graph had greedy sites.)

The usefulness of this decomposition of an avalanche into waves of toppling comes from the fact that the set of all waves is in one to one correspondence with the set of all two-spanning trees [these are two disconnected trees that together span the whole lattice] [38]. In the Potts model formulation these will be the $O(q^2)$ terms in the partition function in Eq. (39). It is sometimes convenient to work in the ensemble in which all waves are given equal weight in determining avalanche statistics. In such an ensemble, we view the evolution of system as a sequence of waves. Given a long time series of waves, say from a simulation, we may ask "what is the probability that in a randomly picked wave in this series, there were s topplings?" This probability will be denoted by $\mathsf{Prob}_w(s)$. Note that in this ensemble, larger avalanches having more waves get more weight.

In two dimensions, it is easily seen that $\mathsf{Prob}_w(s)$ varies as $1/s$ for $1 \ll s \ll L^2$, where L is the size of the system [38]. Dhar and Manna showed that the distribution of the number of sites toppled in the last wave can be related to number of sites disconnected if a bond is deleted at random from a random spanning tree [39]. The latter is expressible in terms of the chemical exponent for spanning trees. Using the known value 5/4 of this in two dimensions, they found that the probability that the last wave in the avalanche has exactly s topplings varies as $s^{-11/8}$ for large s.

7.6. Relation to simple and loop-erased random walks

There is a well-known connection between the resistor-network and spanning-trees problems and simple random walks. This comes from the fact that effective resistance between any two nodes in a resistor network can be expressed in terms of the generating function of simple random walks on the nodes of that graph [40].

Consider a random walk on the vertices of a graph G of N vertices. We imagine the walk to have been going for a long time so that all vertices have been visited at least once by the walker. At any time t, let $e_j(t)$ be the edge corresponding to the direction of last exit of the walker from j, for all j except the position of walker at t. Then clearly, the set of edges $\{e_j(t)\}$ forms a spanning tree on G.

As the walker does a simple unbiased random walk on G, the spanning tree formed by last-exit bonds undergoes a Markovian evolution in time. It was shown by Broder [41] that in the steady state of this Markov process, all spanning trees are generated with equal probability. [The argument is quite straight-forward: it is easy to see that in this Markov process, the transition rate for tree $T \to T'$ is same as the rate for $T' \to T$. Hence, by detailed balance, in steady state all trees occur with equal probability.] We thus have a simple way to generate a uniform distribution of spanning trees on any graph by using simple random walks. Note that using the one-to-one correspondence between the recurrent configurations of the ASM and spanning trees, a time-series of recurrent configurations of ASM obtained by random grain addition and relaxation also gives a (different) time series of spanning trees with uniform distribution.

For any realization of the random walk, it is easy to see that in a spanning tree formed by last exit bonds, the unique path along the tree from the origin to end point of the walk is the loop-erased random walk at that time. Thus the geometrical properties of loop-erased random walks are the same as of chemical paths on spanning trees. In particular, the fractal dimension of loop-erased random walks is 5/4 [42]. One can use this equivalence to relate other properties of loop-erased random walks to those of spanning trees, hence also to ASM's [15]. For example, the probability that the next step of the random walker will result in an erasure of a loop with area s is, in the sandpile language, related to the probability that the last wave will have exactly s topplings. The probability of forming a loop of area 1 in two dimensions is also related to the concentration f_1 of sites of height 1. Let me quote just one more result: If $\mathsf{Prob}_{\mathrm{lerw}}(\ell)$ is the probability that the next step of a loop-erased random walk forms a loop of perimeter ℓ, and $\mathsf{Prob}_{\mathrm{st}}(\ell)$ is the probability that adding a link at

random to a randomly chosen spanning tree will form a loop of perimeter ℓ, then

$$\text{Prob}_{\text{lerw}}(\ell) = \text{Prob}_{\text{st}}(\ell)/\ell. \tag{46}$$

8. The directed abelian sandpile model

The abelian group structure of the original BTW model still does not allow us to deal effectively with the avalanches in the model. The reason is that the avalanche statistics is very 'coordinate-dependent'. For an abelian group generated by two operators $\{a_1, a_2\}$, an equally good choice of generators is $\{a_1 a_2, a_2\}$. But this set will clearly have a different avalanche statistics!

There is a variant of the BTW model, the directed ASM (DASM) that is much more tractable analytically. The model was defined to take into account the fact that under gravity, particles would only fall 'down', and not 'up' [43]; and the existence of preferred direction usually changes the universality class of critical behavior. It has the added advantage that it is mathematically simpler, and allows explicit calculation of various quantities.

The model is defined on a square lattice oriented in the $(1, 1)$ direction, so that bonds are at $45°$ to the edge. Sand grains are added anywhere on the top edge with equal probability. For simplicity, we assume periodic boundary conditions in the horizontal direction (Fig. 10). On each toppling, one grain of sand is transferred to each of the two downward neighbors. Particles leave the system if there is a toppling at the bottom layer.

This model can be described as a 'child playing with wooden blocks on a staircase' [44]. Sitting on the top stair, the child drops the blocks randomly, and when a block lands on another block, both blocks fall to the two adjacent sites at the next step below. This perhaps better models the dynamics of a real sandpile, where most of the sand stays inert inside the pile (playing the role of the staircase), the avalanches only reorganize the surface layer, and the sand falls only downwards in topplings.

The toppling matrix Δ of a directed sandpile is upper triangular. Thus, $\det \Delta = |\mathbf{R}|$ is just the product of the diagonal elements, which is equal to 2^N. Hence all stable configurations are recurrent. However, note that the total number of particles in any layer except the top one is conserved mod 2. Hence the space of recurrent configurations breaks into 2^{M-1} disconnected sectors, where M is the number of layers. If M is large, without
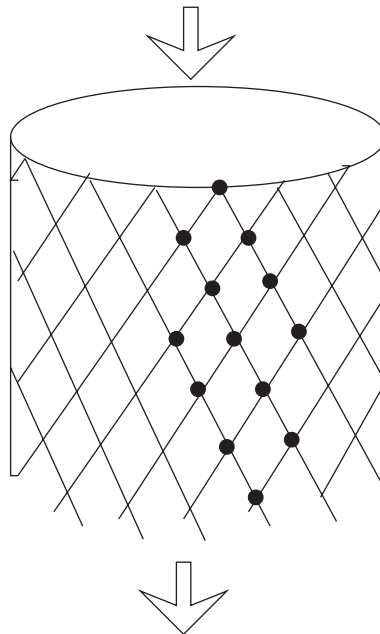

Fig. 10. The lattice structure of the directed ASM. Sand is added and toppled from top to bottom. Periodic boundary conditions are used in the horizontal direction. Note that avalanche clusters have no holes.

significant error, we can consider the invariant measure to be just the product measure of single site distributions, each one having equal probability of having one grain or no grains.

This observation permits a direct calculation of the probability of avalanche sizes. For example, the probability that upon addition of a particle to an arbitrary site at the top of the sandpile nothing happens, is just the probability that the site in question has height 0, namely $1/2$. Thus, we get

$$\mathsf{Prob}(s=0) = \tfrac{1}{2}. \tag{47}$$

The probability to get a single toppling is the same as the probability of having 1 grain in the top site, and no grains in the two nearest neighbors below as in the following diagram, . Here, the filled and open circles denote occupied and empty sites respectively. Hence,

$$\mathsf{Prob}(s=1) = \frac{1}{2^3} = \frac{1}{8}. \tag{48}$$

It is straightforward to continue in this procedure. For $s=2$ avalanches two similar configurations have to be taken into account
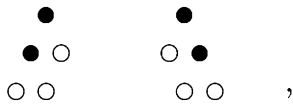
so

$$\mathsf{Prob}(s=2) = \frac{2}{2^5} = \frac{1}{16}. \tag{49}$$

This procedure can be continued for determine $\mathsf{Prob}(s)$ for any finite s. However, explicit enumeration is tedious if s is not very small. We now consider the asymptotics of avalanche size distribution for large values of s. To this end we note that if two neighboring sites in the same level topple, then the site which is directly below both of these sites get two sand grains, and must also topple. This implies that avalanches contain no holes. Therefore an avalanche is completely determined by its left and right boundaries.

Consider the motion of the right boundary as the avalanche progresses downwards. Whether the next step is to the right or to the left, is determined only by the height of the site immediately below and to the right. If the height in question is one, then step is to the right, and if it is zero, it is to the left. Thus, the right boundary, and the similarly the left boundary, are described by simple random walks. The probability that the avalanche stops at the layer Tth layer is the same as the probability that two random walks in one dimension, which start at the same point, meet for the first time after a time T. This is a classical problem in probability, and the probability distribution is well-known [45].

$$\mathsf{Prob}(\text{Avalanche stops at the } T\text{th layer}) = \left(\frac{1}{2T+1}\right)^{2T+2} C_{T+1} 4^{-T-1}. \tag{50}$$

For large T this varies as $T^{-3/2}$.

As an object delimited by random walks, the typical width of an avalanche of duration T scales like $T^{1/2}$, and the typical number of toppled sites scales like $T^{3/2}$. Therefore,

$$\mathsf{Prob}(\text{Avalanche size} > s) \sim \mathsf{Prob}(\text{Duration} > s^{2/3}) \sim s^{-1/3}. \tag{51}$$

Finally the probability of getting avalanche of size s scales like the derivative of the previous expression, namely as $s^{-4/3}$. For a more careful analysis of the generating function of this distribution, see [46].

The directed ASM can be solved exactly in higher dimension as well. For $d > 2$, the boundaries of clusters are not lines, but surfaces. Also, the clusters can have holes. So, we cannot use the simple random walk arguments to determine the exponents. The tools needed to analyze avalanche statistics in this general case are the two- and three-point Green's functions. The simplifying feature of the directed ASMs is that these functions satisfy linear equations. The two point Green's function $G_2(t, \vec{x}|0, \vec{0})$ has already been discussed before: It is the probability of a topple at the site $(t, \vec{x})$ given an addition of grain of sand at $(0, \vec{0})$. Here we

denote by 'time' the coordinate along the down direction, and $\vec{x}$ is a $(d-1)$-dimensional vector giving the position of a site on the constant-t surface.

In the invariant state it is equally likely to have any number between 0 and $d-1$ grains of sand at a given site, and therefore the probability that it topples given that r of its upward neighbors have toppled is r/d. This yields the relation

$$G_2(t, \vec{x}|0, \vec{0}) = \frac{\langle r \rangle}{d} = \frac{1}{d} \sum_i G_2(t-1, \vec{x} - \vec{e}_i|0, \vec{0}), \tag{52}$$

which is a discrete diffusion equation for G_2. Its solution behaves for large t as

$$G_2(t, \vec{x}|0, \vec{0}) \sim \frac{1}{t^{(d-1)/2}} \exp\left(-\frac{\vec{x}^2}{2t}\right). \tag{53}$$

The flux of particles through a surface of equal t scales like t^0 as expected

$$\text{Flux} \sim \int G_2(t, \vec{x}|0, \vec{0}) \mathrm{d}^{d-1}x \sim \text{const.} \tag{54}$$

Let us assume that the probability to have an avalanche of 'duration' greater than t scales asymptotically as $t^{-\alpha}$. The flux relation implies that an avalanche that reaches t has typically t^α topplings there, and therefore the total mass of the avalanche s varies as $t^{1+\alpha}$. It follows that the probability of having an avalanche of size greater than s scales like $s^{-\alpha/(1+\alpha)}$.

To find α we need another independent measure, for example

$$\langle (\text{Flux through } t)^2 \rangle \sim t^\alpha. \tag{55}$$

The expectation of the square flux is expressible in terms of the 3-point function

$$G_3(t, \vec{x}, \vec{y}|0, \vec{0}),$$

which is the probability that both $(t, \vec{x})$ and $(t, \vec{y})$ topple given that one particle was added at $(0, \vec{0})$. G_3 obeys an equation similar to that of G_2,

$$G_3(t, \vec{x}, \vec{y}|0, \vec{0}) = \frac{1}{d^2} \sum_{ij} G_3(t-1, \vec{x} - \vec{e}_i, \vec{y} - \vec{e}_j|0, \vec{0}) \quad \text{for } \vec{x} \neq \vec{y} \tag{56}$$

$$= G_2(t, \vec{x}|0, \vec{0}) \quad \text{for } \vec{x} = \vec{y}. \tag{57}$$

Using Eq. (52), it is easily checked that Eq. (56) is solved by the ansatz

$$G_3(t, \vec{x}, \vec{y}|0, \vec{0}) = \sum_{t'=0}^{t} \sum_{\vec{z}} f(t', \vec{z}) G_2(t, \vec{x}|t', \vec{z}) G_2(t, \vec{y}|t', \vec{z}), \tag{58}$$

where the sum is over all the sites that may be toppled by an avalanche starting from $(0, \vec{0})$. The unknown function $f(t, \vec{z})$ is constructed recursively, so as to satisfy the boundary conditions Eq. (57). Putting $\vec{x} = \vec{y}$ in Eq. (56), we get

$$G_2(t, \vec{x}|0, \vec{0}) = \sum_{t'=0}^{t} \sum_{\vec{z}} f(t', \vec{z}) G_2^2(t, \vec{x}|t', \vec{z}). \tag{59}$$

This equation expresses the known function $G_2(t, \vec{x}|0, \vec{0})$ as a sum of terms linear in $f(t', \vec{z})$ where the site $(t', \vec{z})$ is in the backward light cone of $(t, \vec{x})$. Hence these can be solved recursively for all $f(t, \vec{z})$, starting with $t = 0$.

The flux condition (54) plus the boundary condition (57) yield a sum rule

$$1/d = \sum_{\vec{x}} G_2(t, \vec{x}|0, \vec{0}) = \sum_{\vec{x}, \vec{z}} \sum_{t'=0}^{t} f(t', \vec{z}) G_2(t, \vec{x}|t', \vec{z})^2 \tag{60}$$

$$= \sum_{\vec{z}} \sum_{t'=0}^{t} f(t', \vec{z}) K(t - t') = \sum_{t'=0}^{t} g(t') K(t - t'), \tag{61}$$

where we have defined $g(t) = \sum_{\vec{x}} f(t, \vec{x})$, and $K(t) = \sum_{\vec{x}} G_2^2(t, \vec{x}|0)$. The kernel K is easily calculated in terms of the known G_2 [Eq. (53)], and it scales for large t as

$$K(t) \sim t^{-(d-1)/2}. \tag{62}$$

For $d > 3$, $\sum_t K(t)$ converges, which shows, using the sum rule that $g(t)$ tends to a constant for t large. When $d = 3 \sum_t K(t)$ diverges logarithmically so $g(t) \sim 1/\log t$ and, similarly, in two dimensions $g(t) \sim t^{-1/2}$. Using these results and

$$\langle (\text{Flux through } t)^2 \rangle = \sum_{t'=0}^{t} g(t') \tag{63}$$

then shows that $\alpha = 1$ in dimension $d > 3$. This implies that the probability that avalanche stops at the Tth layer varies as $(\log T)/T^2$. These logarithmic corrections have been verified in simulations [47]. We have already seen that in two dimensions, $\alpha = 1/2$. The upper critical dimension is three.

9. Models of undirected sandpiles

9.1. One dimensional chains and ladders

The simplest undirected model is defined on a one dimensional chain of length L. The matrix Δ is tridiagonal

$$\Delta = \begin{pmatrix} 2 & -1 & & & \\ -1 & 2 & -1 & & \\ & -1 & 2 & \ddots & \\ & & \ddots & \ddots & \end{pmatrix} \tag{64}$$

and its determinant is easily seen to be

$$\det \Delta = L + 1. \tag{65}$$

It is thus a degenerate case where the number of recurrent configurations grows only polynomially and not exponentially with L. It is not hard to identify the $L + 1$ recurrent configurations. They are either a configuration with all ones, or a configuration with a single zero somewhere along the chain.

The result of an addition of a grain of sand at point y to a configuration with a zero at x is as follows: Let us consider first the case $x < y$. The site y is toppled, then its nearest neighbors, and so on, creating a wave which stops on one side at x and at the other side at L. The result of this wave of toppling is a configuration with two grains of sand at y, zero at $x + 1$ and at L, and one grain everywhere else. Now a second wave of toppling begins at y at the end of which the zeros move to $x + 2$ and $L - 1$. This process continues until one of the zeros reaches y and then it stops. The total number of topplings s in such an avalanche is $s(x, y) = (L - x) \min(L - y, y - x)$. The case $x > y$ is similar. We then obtain the avalanche distribution using the fact x and y are uniformly distributed

$$\text{Prob}(s) = \sum_{x=0}^{L} \sum_{y=1}^{L} \frac{1}{L(L+1)} \delta(s - s(x, y)). \tag{66}$$

Details may be found in the paper by Ruelle and Sen [48]. It may be of interest to note that for finite L, the function Prob(s) is not a monotonically decreasing function of s, and shows gaps (depending on L) where Prob(s) is exactly zero. For large L, x and y are of order L, and hence $s = O(L^2)$. Another way to express this is by a direct calculation of the probability distribution of s which takes the scaling form

$$\text{Prob}_L(s) \sim \frac{1}{L^2} f\left(\frac{s}{L^2}\right), \tag{67}$$

where f is a scaling function whose explicit form is known [48]. The gaps in the function $\text{Prob}_L(s)$ are filled by the smearing, and the scaling function f is well behaved. This distribution function has the undesirable feature that in the thermodynamic limit $L \to \infty$ the probability of observing any finite avalanche goes to zero.

This behavior is atypical even for one-dimensional models. For example, on a ladder, or a necklace (a decorated chain) [Fig. 11], we can determine the behavior of successive waves of toppling, and hence the distribution of avalanches [49]. Unlike the linear chain, on a ladder or necklace, the number of recurrent configurations grows exponentially with L. The avalanches are of two types: Type I consist of a single wave which stops after toppling a finite fraction of sites, and Type II which consist of many waves of topplings and
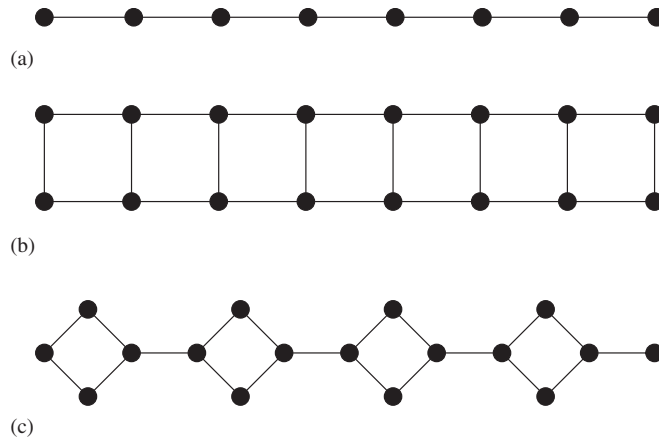

Fig. 11. Some one-dimensional lattices: (a) a simple chain (b) a ladder (c) a necklace.
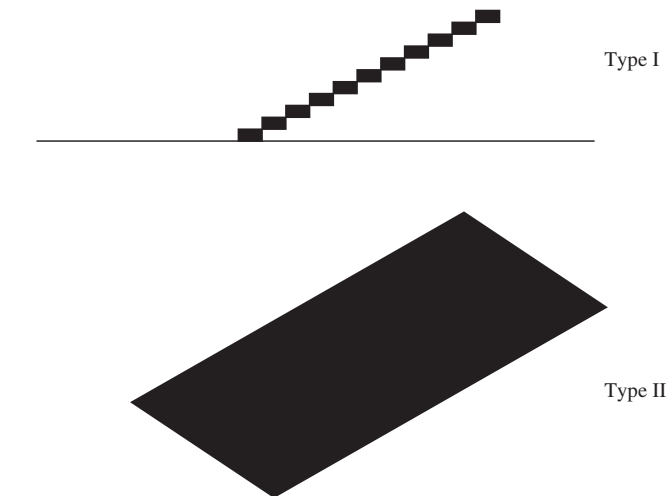

Fig. 12. The space–time evolution of two different types of avalanches on decorated linear chains.

is similar to the avalanches in a single chain (see Fig. 12). Both these types occur with O(1) probability, so that the event size probability distribution takes the asymptotic form

$$\mathsf{Prob}_L(s) \sim \frac{1}{L} f_1\left(\frac{s}{L}\right) + \frac{1}{L^2} f_2\left(\frac{s}{L^2}\right). \tag{68}$$

This linear combination of simple scaling forms is a very simple example of multifractal behavior, with just two exponents. It demonstrates how simple finite-size scaling may be violated.

9.2. The Bethe lattice

Apart from the linear chain and ladders, the only explicitly solvable realization of the undirected sandpile model is when it is defined on a tree, such as the Bethe lattice. As expected, the model displays a mean field behavior on this effectively infinite-dimensional lattice.

I only indicate the general technique of solution. For details, the reader has to consult the original paper [50]. Consider the ASM on a Cayley tree. One starts by characterizing the recurrent configurations. Consider the subconfiguration on a subtree of r generations. The allowed configurations can be divided into two classes: weakly allowed, and strongly allowed. Strongly allowed have no FSC even if it is part of a bigger tree. Let $S_r(z)$ and $W_r(z)$ be the number of such configurations for a subtree with r generations having height z at the top site of the strong and weak type, respectively. It is easy to write down recursion $S_{r+1}(z)$ and $W_{r+1}(z)$ in terms of their values at the rth generation. For large r, these diverge as $\exp(\exp(r))$, but their ratios tend to finite limits. These limits are used to determine the relative probabilities of various subconfigurations deep inside the tree in the steady state. For example, we find that for a 3-coordinated lattice, the sites with heights $1, 2$ and 3 occur with relative frequencies $1 : 4 : 7$. The propagation of avalanches is simple in this lattice. On adding a particle, all sites belonging to the cluster of sites having height 3 containing the point of addition topple, and no other. There are very few multiple topplings. It is then straight forward to write down explicit expressions for $\mathsf{Prob}(s)$ for $s = 1, 2, \dots$.

Unlike the one-dimensional chain, here the probability to get a finite event remains finite in the thermodynamic limit, the and the probability distribution of the number of toppling s behaves asymptotically as $s^{-3/2}$. In fact, the spread of avalanche on the Bethe lattice is very similar to that of infection in a contact process at criticality.

The mathematical treatment simplifies considerably if we consider a directed Bethe lattice, such that the number of 'in' and 'out' edges at every node is equal to n. Then, all stable configurations are recurrent, and the probability that a site catches infection from an infected neighbor is precisely $1/n$, same as in the critical contact process [51]. From the known results about the critical contact process on a tree it follows that $\mathsf{Prob}(s)$ for large s varies as $s^{-3/2}$. Note that we showed that the ASM which belongs to the $q = 0$ Potts model universality class, but on a Bethe lattice, it becomes equivalent to the percolation problem, which actually corresponds to $q = 1$ Potts model.

There are many other treatments of the mean-field theory of sandpiles, all give the same set of mean-field exponents [52].

9.3. The undirected ASM in two dimensions

The undirected ASM on the square lattice is undoubtedly the most studied of the SOC models. Many results are known exactly, but no closed-form expression for the avalanche probabilities, or avalanche exponents.

Let us start by summarizing the known results. Consider a $L \times L$ lattice. The number of recurrent states $|\mathbf{R}|$ is equal to $\det \varDelta$ using Eq. (21). The matrix $\varDelta$ is easily diagonalized by a Fourier transformation, and we get

$$\det \varDelta = \prod_{\ell=1}^{L} \prod_{m=1}^{L} \left[4 - 2\cos\left(\frac{2\pi\ell}{L+1}\right) - 2\cos\left(\frac{2\pi m}{L+1}\right) \right]. \tag{69}$$

This number grows as $\exp(\omega L^2)$ for large L, where ω may be called the entropy per site in the steady state. For large L, we may replace the product by an exponential of an integral, giving

$$\omega = \int_0^{2\pi} \frac{d\theta}{2\pi} \int_0^{2\pi} \frac{d\phi}{2\pi} \log(4 - 2\cos\theta - 2\cos\phi). \tag{70}$$

9.3.1. Height correlations in the steady state

For this case, a fairly detailed characterization of the steady state has been achieved. For example, we may wish to find the probability distribution of the height at a given site, as it determines the probability that there is no toppling if we add a particle. The simplest to calculate is [53]

$$\mathsf{Prob}(z_i = 1) = \frac{\#\{\text{recurrent states in which } z_i = 1\}}{\#\mathbf{R}}. \tag{71}$$

Consider an auxiliary ASM defined on a graph with site i and its connecting links removed. In the burning algorithm, a site with $z_i = 1$ can be burned only after all of its neighbors have been burnt. Let $\mathscr{C}$ be a recurrent configuration of the sandpile with $z_i = 1$. We define $\mathscr{C}'$ to be a sandpile configuration of the auxiliary ASM obtained from $\mathscr{C}$ by deleting the site i, and decreasing the height at each neighbor of i by 1. It is easy to see that burning proceeds identically in $\mathscr{C}$ and $\mathscr{C}'$. Thus there is one-to-one correspondence between recurrent configuration of the original ASM with $z_i = 1$, and all recurrent configurations of the auxiliary ASM. But the latter is easily calculated by the determinant of its toppling matrix, say Δ'.

We augment the toppling matrix Δ' by adding a diagonal entry 1 for the site i. The only rows and columns in which Δ' is different from Δ are those associated with i and its four neighbors. Thus we can write $\Delta' = \Delta + \delta$ where δ has non-zero entries only in a 5×5 sub-matrix. Then

$$\mathsf{Prob}(z_i = 1) = \frac{\det \Delta'}{\det \Delta} = \det(1 + \Delta^{-1}\delta), \tag{72}$$

which boils down to the calculation of a 5×5 determinant. The outcome of this calculation [53] in the limit $L \to \infty$ is

$$\mathsf{Prob}(z_i = 1) \equiv f_1 = \frac{2}{\pi^2}\left(1 - \frac{2}{\pi}\right) \simeq 0.0736. \tag{73}$$

One can also calculate the probability that in the steady state, a randomly chosen site has height 2, 3 or 4. These require a more sophisticated use of graph-theoretical techniques. As this calculation is somewhat involved [54], (even writing down the exact analytical expressions for the final result would take up nearly a page) we only quote the numerical values of the final result here: The density of sites of heights 2, 3 and 4 in the steady state are approximately $0.1739, 0.3063$ and 0.4461, respectively. Interestingly, a high-precision numerical evaluation of different integrals involved, seems to give the average height exactly equal to the simple fraction $25/8$, an observation that deserves a simpler explanation [55].

Similarly it is possible to calculate as a ratio of determinants the joint probability that two sites i and j both have height 1. The calculation now involves calculating the determinant of a 10×10 matrix. If the distance r_{ij} between the sites is large, the leading r-dependence is found to be of the form

$$\mathsf{Prob}(z_i = 1, z_j = 1) \sim f_1^2 + \frac{A}{r_{ij}^4}. \tag{74}$$

[More generally, in d-dimensions, the correlations in heights decay as r^{-2d} with the separation r.] The coefficient A, which may be calculated explicitly, is negative. Thus, the height variables show some anti-correlation. We recall that having two adjacent sites with height 1 is forbidden in the steady state.

Interestingly, the correlations of heights 2, 3 and 4 on the square lattice are qualitatively different. Recently, Piroux and Ruelle have shown that these corrrelation functions are of the form [56]

$$\mathsf{Prob}(z_i = a, z_j = b) \sim f_a f_b + \frac{1}{r_{ij}^4}(A_{ab} \log^2 r_{ij} + B_{ab} \log r_{ij} + C_{ab}). \tag{75}$$

Here A_{ab} is zero if at least one of a and b is 1, and B_{ab} is zero if both $a = b = 1$. The difference in the behavior of probabilities for heights 1 and others comes from the fact that the local operators corresponding to these in the corresponding continuum (logarithmic) conformal field theory are different, and there is a second scaling field whose correlation function varies as $(\log r)/r^2$.

One can also study how the height probabilities are modified near an open boundary. It is found that the probability of height h differs from the bulk value at a distance z from the boundary, by an amount which varies as z^{-2} for $h = 1$, and as $(\log z)/z^2$ for $h \neq 1$ [56].

9.3.2. Avalanche exponents in two dimensions

We now come to the still unresolved question of exponents of avalanches in the 2-d model. The avalanche exponents, which are expected to be universal in two dimensions, are still unknown. The values of numerical estimates made by different people have shown a wide range of values [57], with different methods of analysis giving different values. Avalanche sizes may be measured in terms of different quantities, such as the total number of topplings s, the number of distinct sites toppled s_d, the radius R of the affected area, the 'duration' T of the avalanche, and n_w, the number of waves in the avalanche.

In the simple finite-size scaling picture, one assumes that the different measures are related to each other by simple scaling, and given the diameter of avalanche R, other measures scale as simple powers of R. In this case, we would expect that

$$\mathsf{Prob}(R) \sim r^{-\tau_r} f(R/L), \tag{76}$$

where L is the size of system.

From the compactness of avalanche clusters, it follows that s_d scales like R^2. From the Potts model equivalence, we see that the time T needed to reach a site of distance R from the origin of the avalanche scales as the chemical length of the path, so that $T \sim R^{5/4}$. If τ_s, τ_d, τ_r and τ_t are the exponents characterizing the distributions for s, s_d, r and T, this implies that

$$\tau_r - 1 = 2(\tau_d - 1) = \tfrac{5}{4}(\tau_t - 1). \tag{77}$$

If we assume that n_w scales as a power of r, say as r^y, then, s varies as $n_w s_d$, and hence as r^{2+y}. To determine the avalanche exponents, we use two relations: $\langle s \rangle \sim L^2$, and $\langle n_w \rangle \sim \log L$. These immediately give us

$$\tau_r = y + 1, \quad \tau_s = 2(1 + y)/(2 + y). \tag{78}$$

Thus all the exponents are determined up to the single parameter y. Priezzhev et al. using some identification of known scaling dimensions of the two-dimensional Potts model, have conjectured [58,59] that $y = 1/2$ which leads to $\tau_d = 5/4$ and $\tau_s = 6/5$ (where τ_s is the power-law decay of the s distribution), which is roughly consistent with the numerical results.

However, the simple scaling assumption cannot be correct, as there will surely be multiplying logarithmic factors in various functions, [e.g. Eq. (76)]. But more importantly, simulation studies of De Menech et al. [60], have shown that avalanches that reach the boundary have a qualitatively different scaling behavior than those that do not dissipate particles. Their analysis of numerical data suggests that the fractional number of avalanches whose radius exceeds r decreases as $r^{-1/2}$, for $r \gg 1$. The avalanches that do not reach boundary have $s \sim s_d$ and $n_c \sim 1$. For a lattice of size L, only a fraction $L^{-1/2}$ of the avalanches reach the boundary, but those that do, typically have $L^{1/2}$ more waves, so that the average size of avalanches that reach boundary is $L^{5/2}$. Thus, according to these authors $y = 1/4$ for dissipative avalanches, but $y \approx 0$ for the non-dissipative ones. Tebaldi et al. use multifractal formalism to analyse their data [61], but it seems possible that the simpler the linear combination of two scaling forms discussed earlier [Eq. (68)] provides an adequate description.

We have already mentioned that the probability of last wave of size s varies as $s^{-11/8}$. This also implies the upper bound $\tau_s \leqslant 11/8$. Another exact result known is the distribution of size of a wave generated at the corner of a wedge of angle θ, with particles allowed to leave system at boundaries. In this case, Priezzhev et al. showed that the probability of avalanches of size s varies as $s^{-\tau(\theta)}$, where $\tau(\theta) = 1 + \pi/2\theta$ [62]. For a boundary avalanche, this gives $\tau(\pi) = 3/2$.

The scaling picture of avalanches has been extended to study correlations between successive waves of toppling [63]. From numerical simulations, it is seen that the conditional probability $\mathsf{Prob}(s'|s)$ that the

$(k+1)$th wave is of size s', given that the previous wave had s topplings is roughly independent of k. This varies as $(s'/s)^a A(s)$ for $s' \ll s$, and as $(s'/s)^{-b} B(s)$ for $s' \gg s$. Here $A(s)$ and $B(s)$ are some s-dependent amplitudes. However, the range of validity of these power-laws is limited to $1 \ll s, s' \ll L^2$.

9.4. Avalanche exponents in three dimensions

The undirected BTW model in $d=3$ is actually simpler than the $d=2$ model, in that here multiple topplings occur with much smaller probability, and can be neglected. This implies that $s \sim s_d$. Simulations by Ktitarev et al. [64] have also shown that holes in the avalanche clusters are unimportant, so that $s \sim s_d \sim R^3$. For individual waves, the finite scaling works very well. The probability distribution of avalanche having s topplings on a lattice of linear size L is expected to have the scaling form

$$\text{Prob}(s|L) \sim s^{-a} h\left(\frac{s}{s^*(L)}\right), \tag{79}$$

where the scaling function $h(x)$ tends to a constant for small x, and tends to zero fast for large x. Using the compactness of avalanche clusters, the cutoff value $s^*(L)$ must vary as L^3. Then, in order to have $\langle s \rangle \sim L^2$, we must have $a = 4/3$. This implies that

$$\tau_s = \tau_d = \tfrac{4}{3}. \tag{80}$$

As a check on the scaling theory, note that the probability that avalanche reaches a distance R scales as the probability that number of topplings is greater than R^3, hence as $1/R$, which also agrees with the known result about expected number of topplings at a distance R.

The only exponent which this simple argument does not give is the exponent for the duration of avalanches. But the propagation of avalanches occurs along spanning trees path in the equivalence between the sandpile model, and the duration T of an avalanche must vary as R^z, where z is fractal dimension of chemical paths of spanning trees in three dimensions. This has been estimated numerically recently using simulations of LERW's [65], giving $z = 1.6183 \pm .0004$. This implies that the probability that the duration of avalanche is greater than T varies as T^{-y}, where

$$y = 1/z = 0.6179 \pm 0.0002. \tag{81}$$

Analytical determination of z remains an open problem.

9.5. Higher dimensions

For the undirected ASMs in higher dimensions, it was shown by Priezzhev [66] that the upper critical dimension is 4. He used the equivalence to the loop-erased random walk problem, and the fact that the upper critical dimension is 4 for intersections of paths of random walkers. For $d > 4$, the exponents take the mean field values.

10. Models related to the directed sandpile model

In Section 7, we studied the directed ASM (DASM) as an example of a self-organized system in which the invariant state is easily characterized, and all the avalanche exponents can be determined exactly, in all dimensions. The model is also equivalent to other statistical models which were proposed in other contexts. Here I will discuss three such models.

10.1. Scheidegger's model of river basins

The first is the Scheidegger's model of river basins [67]. Scheidegger, a hydrologist, originally proposed this model as a very simplified description of how rainfall accumulates into small streams which then join to become larger and larger rivers. We consider a large area with roughly uniform average rainfall, and having a constant average slope (say southward). We represent the area approximately as a square grid, tilted and
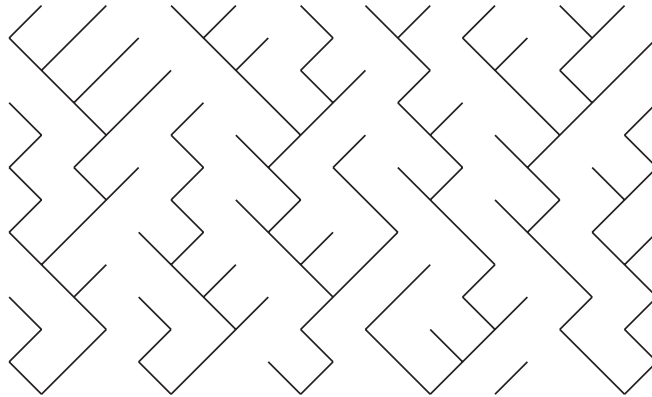
Fig. 13. The Scheidegger model of a river network.

oriented as in the DASM. At any point of the lattice, there may be zero, one or two streams of water bringing water from its two north–east and north–west neighbors. If n units of water come into a site per unit time (usually taken to be a year in geophysics), $(n + 1)$ units of water leave the site in a single stream towards one of the two sites just below it (the extra one unit comes from the local rainfall). Whether it goes to the south–east or south–west neighbor depends on local geographical details. In this model, these directions are chosen randomly at each site.

If we draw the directions of water-flow going out of each site, we get a picture of the river network of the area. Such networks are also called drainage networks. In a drainage network, there is a unique path from each site to the 'sea' (the lower boundary in Fig. 13). Also, there are no loops, if we ignore the possibility of a single stream breaking into two streams (fairly good approximation away from delta regions), the drainage networks must form a directed spanning tree.

Using these rules it is now possible to calculate the probability that the outflow from a site is one unit: This event happens if and only if the site receives no water from either of its two up neighbors, because the right-hand side neighbor has outflow directed to the right, and the left neighbor is flowing to the left. Thus $\mathsf{Prob}(\text{outflow} = 1) = 1/4$. Similarly, to get an outflow of two units, it is necessary to have inflow of one unit, so that one of neighbors from above has to have outflow of 1 directed at the given site, and the other neighbor from above has to have outflow directed to its other neighbor from below. Such an event has probability 1/16, and since there are two ways to choose the flow into the site, we have $\mathsf{Prob}(\text{outflow} = 2) = 1/8$.

On comparing the previous argument with the discussion of the DASM we see that the configuration of sites required to get an outflow of two units is identical to that which is associated with an avalanche of size two, starting from the given site and going *upwards*. The two configurations which are associated with outflow of two units are the ones possible for a size two avalanche, and a similar result holds for larger values of the outflow. The only difference is that there is no possibility of outflow of zero units. Therefore we have the relation

$$[\mathsf{Prob}(\text{outflow} = s)] = 2[\mathsf{Prob}(\text{DASM avalanche size } = s)] \quad \text{for } s > 0. \tag{82}$$

Now all the earlier discussed results regarding the DASM apply equally well to the river network model. In particular, a river of total length ℓ will drain typically an area of size $\sim \ell^{3/2}$. This observation is in rough agreement with observation on rivers on scales which are not very large.

We can study the model in higher dimensions. In three dimensions, one can think of the capillary network for flow of blood in an animal, where each 'cell' generates 'waste', which has to be transported out using the tree-like network of capillaries. Drainage networks in higher dimensions are harder to visualize.

The Scheidegger river network model in fact generates a directed spanning tree of the lattice. When the river network is situated in a relatively flat landscape, it should resemble more an undirected spanning tree, so a simple model for such a network would be just to assume that in a river network on a flat landscape, all spanning trees are equally likely to be realized. *The geometrical structure of river networks on nearly flat land*

can be modeled by that of a random spanning tree in two dimensions. It turns out that this simple model describes the real river networks just as well as the more complicated models proposed in literature.

The random spanning trees are described by the 0-state Potts model. Using the results from the conformal field theory for Potts model, we see that for random spanning trees, the typical length L of the path along tree between two points at a Euclidean distance R scales like $L \sim R^{5/4}$. This scaling provides an estimate of the area A drained by a river of length L

$$A \sim R^2 \sim L^{8/5}, \tag{83}$$

that is, slightly larger than the exponent in the directed network (where $A \sim L^{3/2}$).

There is a large amount of literature dealing with the modelling of river networks. If we include the phenomena of erosion, which transports matter, and thus alters the elevation across the landscape, which in turn affects the river-flow, we have a complex self-organized structure. A long excursion into models of river networks is outside the scope of these lectures. I will only provide a few pointers here [68].

10.2. Takayasu's model of diffusion with aggregation

We have already defined the model in Section 3.3. It is not hard to see that this model in one dimension is same as the (two-dimensional) river network model. We consider a space-time history of the evolution. The world-lines of a diffusing particles look like the rivers of Fig. 13. The probability to have a particle a mass M is therefore equal to the probability to have outflow M, which is twice the probability of finding an avalanche of size M in the respective DASM. Therefore, for large t, the mass probability distribution is characterized by the same exponent

$$\mathsf{Prob}(M) \sim M^{-4/3} f\left(\frac{M}{M^*(t)}\right), \tag{84}$$

where $M^*(t)$ varies as $t^{3/2}$, and f is some cutoff function. This model is also easily generalized to higher dimensions.

10.3. The voter model

The voter model is defined as follows: we consider a d-dimensional lattice. At each site, there is an individual (voter) who has an opinion on an issue. We take this opinion to be a two-valued discrete variable (yes or no). A voter can communicate with his neighbors, and can change his opinion in time. We take time-evolution to be discrete time Markovian: if at time t, a site has exactly r neighbors who vote yes, at time $t + 1$ this site would choose to vote 'yes' with probability $r/(2d)$, and 'no' with probability $1 - r/(2d)$.

Given the particular choice of local transition rates, one can try to write down evolution equations for ensemble averaged quantities, for example $\langle \eta(x, t) \rangle$, where $\eta(x, t)$ specifies state of the voter at site x at time t, taking value 1 if 'yes', and 0 if 'no'. Normally, such evolution equations involve higher-order correlation functions. This gives the well-known BBGKY hierarchy of equations for correlation functions. It is easy to see that for the voter model, this hierarchy closes on itself. The equation for evolution of $\langle \eta(x, t) \rangle$ involves only the $\langle \eta(x', t) \rangle$ at neighboring sites x', and no higher order correlation functions. Specifically, in two dimensions

$$\langle \eta(x, t + 1) \rangle = \frac{1}{4} \sum_{x'} \langle \eta(x', t) \rangle, \tag{85}$$

where the sum over x' is over the nearest neighbors of x. These are linear equations, easily solved by eigenmode decomposition. One can similarly show that equations satisfied by the 2-point correlation functions also close on themselves, and so on. This model has been studied a lot, and a fair amount of literature exists about it [69].

To note the connection with the directed ASM, consider evolution of a d-dimensional voter model which at time $t = 0$ has only one voter having a 'yes' vote in a sea of 'no's. Then in the space-time history of the evolution, there is a single cluster of 'yes' sites. It is easy to see that the probability that this cluster will have a given shape is exactly the same as that of the same avalanche cluster in the DASM in $(d + 1)$ dimensions.

11. The abelian distributed processors model

It is useful to see how far ASM can be generalized, still retaining its abelian group structure. In this section, I shall discuss an interesting generalization of the ASM. The model consist of a network of nodes and links (a graph), on whose nodes sit processors, which are finite state automata. Each of these has an input stack of messages. When the input stack of a processor is not empty, it pops one of the messages according to a predetermined order, and processes it. As a result of the processing its internal state may change, and some messages may be transmitted to its neighbors in the network, or to the outside world, using the outgoing links from that site. Then if the input stack is still not empty, the next message is processed, otherwise the processor idles. The processing rules for different processors may differ.

In many applications, especially in computer science, one considers such networks where the speed of the individual processors is unknown, and where the final state and outputs generated should not depend on these speeds. Then it is essential to construct protocols for processing such that the final result does not depend on the order at which messages arrive at a processor. If this is indeed the case, the node may be said to have the abelian property. It is then easy to show that a network of nodes, all of which have abelian property, also has abelian property. This model is named an abelian distributed processors (ADP) model.

Evidently, the ASM is an example of the ADP model where the local processor stores incoming messages, and once the number of stored messages exceeds a threshold, distributes them to specified other processors. Another condition which has to be imposed on an ADP is the equivalent of the 'good behavior' conditions for the ASM. Namely, that the response of the network to a single message sent to any of the processors terminates in a finite time, after which all the processors sit idle until further input is applied. The state in which all processors are idling, and all input stacks are empty is called a quiescent state. The quiescent states are the analogs of the stable configurations of the ASM.

As in our discussion of the ASM, one may define generators $a_{i,m}$ whose action is to send message m to processor i. These generators commute, and generate an Abelian semi-group, acting on the set of quiescent states; restricted to the set of recurrent states, they form an abelian group.

11.1. The Eulerian walkers model

For example, consider a sandpile model in which the toppling rules at each site change from toppling to toppling. As a particular case, the rule governing toppling at a site may be assumed to be a periodic function of the number of topplings already occurred *at that site*. The simplest of such models is the Eulerian walkers model [70]: Consider a square lattice of size $L \times L$. On each site sits an arrow pointing toward one of the four directions: north, south, east or west. A walker is placed on the lattice at one of the sites. The walker reaching a site resets the direction of the arrow at that site by rotating it by $90°$ clockwise, and takes a step to the neighboring site in the new direction. It repeats this action, till it leaves the lattice. In the ASM terminology, here $z_c = 0$, and in a stable configuration, there are no particles. the SOC dynamics generates non-trivial long-ranged correlations between directions of arrows.

We add a walker at a randomly chosen site, wait till it leaves the system, and then add another walker. It is easy to see that this model is an example of the ADP model. We can define commuting operators $\{a_i\}$ whose action on a configuration of arrows results in a new configuration of arrows obtained by adding a walker at i and allowing it to move till it leaves the system. In fact, the algebra of the operators a_j of introducing a walker at site j is (Fig. 5)

$$a_j^4 = a_{j_1} a_{j_2} a_{j_3} a_{j_4}, \tag{86}$$

which is the same as Eq. (5) for the ASM on a square lattice. Therefore we can apply the variation of the script test to see if a particular configuration is recurrent. However, there is a much simpler characterization possible in this case: in a recurrent configuration the arrows form a directed spanning tree on the lattice, all arrows directed towards the sink site.

Although the operator algebra is identical, the avalanches of this model are different from those of the ASM. Since the configuration does not become quiescent before the walker leaves the system, the typical

avalanche size is $O(L^2)$ in contrast with the $O(L^0)$ avalanches which are most likely in the ASM. Thus we see again that the group structure of the algebra of operators cannot by itself determine the avalanche exponents. Avalanches in this model were studied numerically by Shcherbakov et al. [71].

Several quantities of interest in this model have been studied. On an $L \times M$ torus, such a walker eventually ends up in a limit cycle, whose period is exactly $4LM$, and it traverses each bond of the lattice exactly twice in one cycle, once in each direction. Such a tour of the lattice is called an Eulerian circuit, hence the name of the model. If a walker starts at origin in an initially random configuration of arrows, it reorganizes the arrows as it moves, until they form an Eulerian circuit. In dimension $d \leqslant 2$, it revisits the already visited sites many times. The average number of distinct sites visited up to time t increases as $t^{d/(d+1)}$ for $d \leqslant 2$ and as t for $d > 2$.

To make the connection to the ASM more explicit, consider a model in which we drop walkers on a square lattice with an arrow at each site. Each walker waits at the site till the number of walkers waiting at a site becomes greater than or equal to r, and then r walkers leave the site in consecutive clockwise directions, and the arrow is reset. The case $r = 1$ corresponds to the Eulerian walkers model. The case $r = 4$ corresponds to the ASM. In this case the arrow is always reset to the same direction, and it does not matter which way. Thus, we may forget about the arrows, and recover the ASM. For $r > 1$, most of the avalanches are finite, and the probability distribution of avalanche sizes shows a power-law tail. The exponents of the avalanche distribution do not seem to depend on r, so long as it is greater than 1.

In the case $r = 2$, in a quiescent configuration, the number of stable configurations is 8^N for a lattice with N sites (at each site, there are four orientations of the arrow, and 0 or 1 walkers). However, at each toppling, the arrow is rotated by $180°$, and hence alternates between two orientations. This implies that the configuration space breaks into 2^N disconnected sectors of 4^N configurations each, and the largest eigenvector of $\mathscr{W}$ is 2^N-fold degenerate. The steady state is not unique. Even macroscopic quantities like the mean density of walkers in the steady state are weakly sector dependent, but the critical exponents seem to be universal.

The $r = 2$ model has been studied on a 4-coordinated Bethe lattice by Shcherbakov and Turcotte [72]. They calculated the exact probabilities that adding a particle produces 0, 1 or 2 topplings. The calculation for larger s is straight forward, but rather tedious. The avalanche exponents are difficult to determine exactly, but expected to be same as in the mean-field theory.

11.2. The Manna model

Another important class of models which falls in the ADP category, is of sandpile models with stochastic toppling rules. The first model of this type was studied by Manna [73]. In this model, the toppling rule was that if any site has more than one grain it is unstable, and topples. In a toppling, *all* grain at the unstable site are transferred to neighbors, the direction in which a particular grain is transferred is chosen *at random*, independently for each grain.

A variation of these rules is that if the local height at the site exceeds 1, *only two* grains are transferred to randomly chosen neighbors in a single toppling. If the site starts out with many grains, it can undergo multiple topplings. It is easy to verify that this variation makes the model abelian [12]. We need only note that this model can be thought of as an ADP model with a pseudo-random number generator (PRNG) at each node. After each toppling, a new random number is drawn from the local PRNG, and its outcome is used to decide the toppling threshold and the number of grains to be transferred in different directions. As the PRNG's are actually deterministic, the abelian property follows immediately.

We can, however, also think of the local PRNGs as unobservable so that the operation of toppling appears as random. The action of the operator a_i of adding a grain of sand to a basis vector $|\mathscr{C}\rangle$ corresponding to a stable configuration $\mathscr{C}$ does not yield a unique configuration, but a number of different final configurations with different probabilities. Thus $a_i|\mathscr{C}\rangle$ is not another basis vector $|\mathscr{C}'\rangle$, but a *linear combination of basis vectors*. The different operators a_i however still commute.

The closure relations satisfied by the operators a_i, on the square lattice become (Fig. 5)

$$a_j^2 = (1/16)(a_{j1} + a_{j2} + a_{j3} + a_{j4})^2. \tag{87}$$

Product of a_j's can be expressed as (in this case quadratic) polynomial in a's. However, we can not define a^{-1}, even if we restrict to the space of recurrent configurations, as we cannot rule out zero eigenvalues of a's. We thus have to work with a abelian ring, and not an abelian group. As before, we can simultaneously diagonalize all the a's, and the eigenvalues satisfy coupled polynomial equations. Finding explicit solutions is not possible in the general case, unlike the simpler case of deterministic ASM, where only linear equations were encountered.

For the abelian Manna model, where the operators satisfy Eq. (87), one can take the square root of both sides of the equation, and reduce the problem to the linear equations

$$\eta_j a_j = (1/4)(a_{j1} + a_{j2} + a_{j3} + a_{j4}), \tag{88}$$

where $\eta_j = \pm 1$, and the 2^N distinct choices of $\{\eta_j\}$ give us the 2^N different solutions. The structure of these equations is that of the wavefunction of a quantum mechanical particle in a random potential, the random potential at site j being η_j, for a particular energy eigenstate of eigenvalue 0. This thus gets related to the localization properties of the eigenfunctions of the well-known Anderson localization problem [74] for states near the center of the band.

12. Time-dependent properties

Though an explanation of $1/f$ noise was one of the main motivations for the initial proposal of SOC, time-dependent properties of self-organized critical systems have not been studied much theoretically so far. Two types of correlations should be distinguished: within a single avalanche, and over time scales greater than the interval between successive particle additions, which measures correlations between avalanches. For the latter case, while a power spectrum of mass-fluctuations of $1/f$ type has been found in some one-dimensional models [75,76], initial studies suggested that in higher dimensional sandpile models, the behavior is $1/f^2$ [77]. However, more recent estimates of the power-spectrum of activity fluctuations in time in the BTW model gives an exponent less than 2 [78].

More generally, to determine the time-dependent properties of systems with Markovian evolution, one needs to diagonalize the evolution operator. The eigenvalues of the Markovian evolution operator $\mathscr{W}$ were already determined in Section 5.6. Using these, one can easily see that the longest relaxation time for an ASM on a d-dimensional hypercubical lattice varies as L^d. Calculation of time-dependent height–height correlation functions is not easy, as the matrix-elements of eigenvectors are very complicated in the configuration basis.

One remarkable case where the relaxation spectrum is easy to calculate is the one-dimensional Oslo ricepile model [80]. It is a one-dimensional model with stochastic toppling rules defined as follows: Let z_i be the height at site i of a one dimensional lattice $i = 1$ to L. The toppling rule is whenever $z_i - z_{i+1} > \sigma_c(i)$, one grain is transferred from site i to $i + 1$. After each toppling at any site j, the critical threshold $\sigma_c(j)$ is reset randomly to a new value 1 or 2, with probabilities p and $1 - p$, respectively. Particles are added one grain at a time at the left end, and leave from the right end.

It is easy to check that the model is abelian, and this is a special case of the ADP model. Let a_1 be the operator corresponding to adding a grain at the left end. Then from the operator algebra for this model, it is easy to show that [79]

$$a_1^{L(L+1)+1} = a_1^{L(L+1)} \quad \text{for all } p. \tag{89}$$

As in this case $\mathscr{W} = a_1$, this equation has the remarkable consequence that eigenvalues of $\mathscr{W}$ are either 0 or 1. Also, as one can show that all recurrent configurations are reachable from any other, and there is a unique steady state for this Markov process, there is only one eigenvector of $\mathscr{W}$ with eigenvalue 1. Thus all the other eigenvalues of $\mathscr{W}$ are 0.

One can still have nontrivial time-dependent correlation functions of different observables, as the matrix $\mathscr{W}$ is not hermitian. However, it follows from Eq. (89) that the time-dependent correlation function $\langle X(t + \tau)Y(t)\rangle = C_{XY}(\tau)$ must be exactly zero in the steady state for all observables X and Y, and all $\tau > L(L + 1)$.

Another question concerns the distribution of residence-times of grains in piles. This has been studied experimentally in piles of rice by the Oslo group [80]. The residence times in the BTW-like models have been studied in [81]. To study residence times, one has to mark a grain, and study its trajectory as it leaves the pile.

But even if only one grain is marked, the model is no longer abelian! However, if we assume that on each toppling, the four transferred particles go in randomly chosen directions, the *path* of the grain is a simple random walk. The nontrivial part comes from the nontrivial waiting times between jumps.

It is see that the first moment of the distribution of residence times is the average mass of the pile. Define a variable $\eta(i,j)$ as the indicator function that the ith grain is in the pile at the end of time step j. Then, $\sum_j \eta(i,j)$ gives the residence time of particle i, and average over i gives the mean residence time. Conversely, $\sum_i \eta(i,j)$ gives the mass of the pile at time-step j, and average over j gives the mean mass of the pile.

While the mean residence time of a grain in a pile of size L in d-dimensions is $\mathcal{O}(L^d)$, the typical distance moved by a grain in a single avalanche is of order 1. If one coarse-grains the diffusive motion of the grain over time-scales $1 \ll t \ll L^d$, then one can define an effective jump-rate out of site i which is proportional to the average number of topplings at i. Then, the probability density $P(\vec{R}, t)$ that the diffusive grain is at $\vec{R}$ at time t satisfies the evolution equation

$$\frac{\partial}{\partial t} P(\vec{R}, t) = K \nabla^2 [n(\vec{R}) P(\vec{R}, t)], \tag{90}$$

where K is some constant, and the average number of toppling per particle $n(\vec{R})$ can be obtained in terms of the density of particle addition $r(\vec{R})$ by solving the particle conservation equation $\nabla^2 n(\vec{R}) = r(\vec{R})$.

For the special case that $r(\vec{R}) = $ constant, Eq. (90) is solved by noting that then $P(\vec{R}, t)$ is independent of $\vec{R}$, and a simple exponential function of time. Integrating $P(\vec{R}, t)$ over $\vec{R}$, we see that the distribution of residence time of grains in the pile is a simple exponential function of time. The unknown constant K can be determined using the condition that the first moment of the distribution gives the mean mass of the pile. The probability distribution for the residence times in terms of the reduced variable $\tau = t/\langle T \rangle$ becomes

$$\mathsf{Prob}(\tau) = \exp(-\tau). \tag{91}$$

Interestingly, the behavior is very different in models where the toppling threshold condition is on the slope, and not on the height. Here, the tail of the distribution of residence times is dominated by grains that get deeply buried in the pile. In the Oslo model, with grains added at one end, if a grain is added when the height of the pile h has fluctuated to a value much lower than the average, it will typically get buried, and stay buried till the height at the height returns to a value h again. The average duration between successive returns to value h clearly varies as 1/Prob(h). Thus the probability that residence time is greater than 1/Prob(h), is proportional to the probability that the height of pile at the time of addition was h or lower, which varies as Prob(h). Equivalently, we get that the probability of residence time is greater than T varies as $1/T$. A more careful analysis shows that there is a logarithmic correction factor

$$\mathrm{Prob}(\text{Residence time} > T) \sim \frac{1}{T(\log T)^x}, \tag{92}$$

where x can be different for different models. It was shown in [82] that the upper cutoff for the distribution of residence times varies as $\exp(L^{d+2})$, for the Oslo model in d dimensions, and not as a power-law in L.

If in the ASM, the particles are not added at random, but in a correlated manner, the noise spectra are changed, and can show $1/f$ behavior [83]. There is also evidence of aging in the probability distribution of the first return times of activity at a site toppled in a large avalanche [84].

13. The generic behavior of sandpiles

The behavior of sandpile-like models seems very confusing, given the large number of different models already defined (and many more could have been), each with its own set of critical exponents. We now try to address the question of universality of critical behavior of sandpile models [85].

A very general paradigm in non-equilibrium statistical physics is directed percolation (DP), which describes the inactive–active state phase transition in a wide class of reaction–diffusion systems [86]. The activity in avalanches can grow, diffuse or die, and any stable configuration is an absorbing state. Thus, one would expect that sandpiles should belong to the universality class of active-absorbing state transition with many

absorbing states [87]. The main question is if the presence of the conservation law of sand makes the critical behavior different from directed percolation.

We have recently argued, but not proved, that as long as the sand-grains have non-zero "stickiness" (i.e., there is small probability that incoming particles to a site get stuck there, and do not cause any topplings), the distribution of avalanche sizes follows directed percolation exponents [88]. The deterministic ASM, and the stochastic Manna models are unstable to this perturbation, and the renormalization group flows are directed away from them to the directed percolation fixed point (Fig. 14). The informal terminology "stickiness" is used here, as a precise identification of the relevant operator has not been made yet.

Let us consider generalizing the directed model of Section 7, and make the toppling rules stochastic. We consider the same lattice as in Fig. 8, with particles added at the top, but change the toppling rule to the following: At each site i, there is a non-negative integer height variable h_i. Initially all h_i are zero. A site becomes unstable at time t, if at least one particle was added to it at the previous time-step, and its height becomes $\geqslant 2$. An unstable site i relaxes at the next time step stochastically: With probability $(1 - p)$, the added grains just stick to the existing stack, and it becomes stable without losing any grains. Otherwise (with probability p), the relaxation occurs by toppling in which the height at the site decreases by two, and the site *becomes stable*. We introduce bulk dissipation by introducing a probability δ that both grains from the toppling are lost, otherwise (with probability $1 - \delta$), the two grains are transferred to the two downwards neighbors of i.

Note that there is a non-zero probability that a stable site can have arbitrarily large number of grains. The model is no longer abelian, and we choose to relax all the unstable sites by parallel dynamics. Once a site has relaxed, it remains stable whatever its height, until perturbed again by new grains coming to the site. This relaxation process is repeated until all sites become stable, and then a new grain is added. We have already studied the special case $p = 1, \delta = 0$ in Section 7.

In this case, it is easy to see that a steady state is possible only if p is not too low, else there is a pile-up of particles near the top layers. The boundary between these two types of behavior is shown in Fig. 15.

This model can be solved exactly along the three boundaries $p = 0$, $p = 1$, and $\delta = 1$. The case $\delta = 1$ is trivial, as no particle reaches the second layer.

If $p = 1$, with δ arbitrary, the only allowed height values are 0 and 1, and all stable configurations are equally likely. In this case, it is easy to generalize the earlier treatment for $\delta = 0$, and show that the n-point correlation functions satisfy linear equations. We omit the details here. The distribution of avalanche-sizes has an exponential decay for non-zero δ.

When $\delta = 0$, the critical value of $p = p^*$ below which no steady state is possible has to be the directed percolation threshold for site percolation on the square lattice. We note that avalanche propagation in this problem is bounded by that in directed percolation (DP), as any site which has some unstable neighbors above, can only be unstable with probability at most p. Then if $p < p_c$, the probability that an avalanche reaches a distance d below top decreases exponentially with d, and a pile-up near top must occur. Conversely, if $p > p_c$, and there is large density of particles at the top, the avalanche cluster will be supercritcal DP clusters,
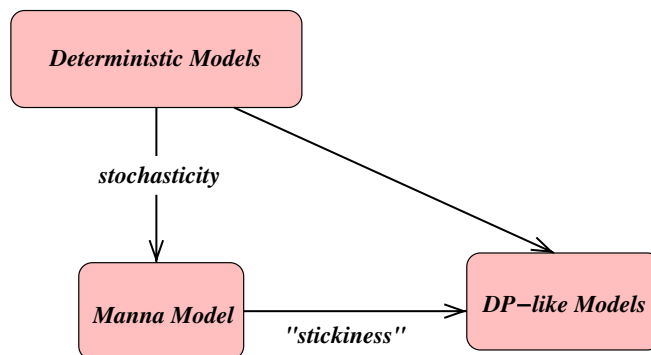

Fig. 14. A schematic flow diagram of the renormalization group flows between different fixed points of the sandpile models.
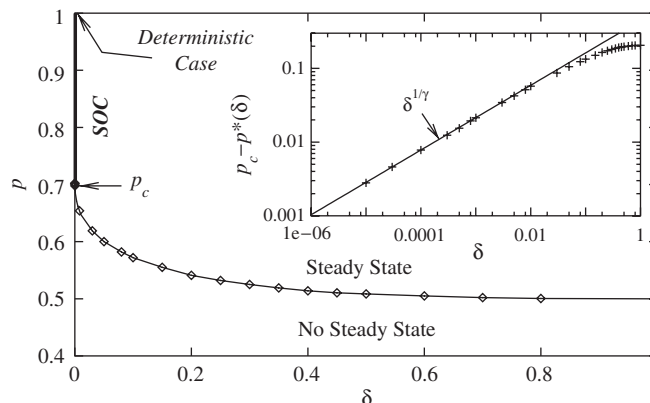
Fig. 15. The line $p = p^*(\delta)$ separating the steady-state and no-steady-state regions in the $p-\delta$ plane. The inset shows the plot of $[p_{c,DP} - p^*(\delta)]$ versus δ. The straight line shows the theoretical slope $1/\gamma$ using known directed percolation value of the exponent γ.

and on the average, grow as they move down, thus removing particles from the top and reducing the density there, and a steady state will exist.

For small δ, the critical boundary $p^*(\delta)$ is given by the requirement that, in the steady state, on the average loss rate should equal the gain. Since number of topplings per avalanche would vary as $(p_c - p)^{-\gamma}$, where γ is the conventional DP exponent, we must have $p_c - p^*(\delta) \sim \delta^{1/\gamma}$. This is verified in the simulations very well (Fig. 15).

For p not near p_c, but $\delta = 0^+$, in the steady state, the growth of avalanche is as in the Domany–Kinzel model of directed percolation, with probabilities p_1, p_2 denoting toppling probability at a site when it get one or two particles respectively. As argued above, in the steady state these are self-organized to be on the critical line of the Domany–Kinzel model, and avalanche clusters are DP like. Our numerical data is fully supporting this picture. We have checked that this behavior is robust against several changes of the toppling rules (allowing both particle to go to same down-ward neighbor, allow multiple topplings, etc.).

The argument is easily generalized to higher dimensions, and directed sandpiles in d-dimensions have the exponents of DP-clusters in d-dimensions. In fact, it can be extended to undirected sandpiles with sticky grains also. In this case, the time-history of topplings in a d-dimensional pile forms an avalanche cluster in $(d+1)$-dimensions, which behaves like critical DP-clusters in $(d+1)$-dimensions. The main difference from the directed case occurs because of the correlations in heights in the time direction in the undirected problem. Again, this does not matter much, because the toppling probabilities do not depend on the precise value of height at a site, only on if it zero or not. And near the phase boundary, the fraction of sites with zero height goes to zero. Our numerical data [88] is in excellent agreement with these theoretical arguments.

That non-zero stickiness makes the avalanche clusters like critical DP clusters can be rationalized this way: Non-zero stickiness means that grains can be lost or join an avalanche, as it traverses the medium. As the grains once they stick at a site, can only come into play again at the next avalanche, in effect, there is no conservation of grains within an avalanche. Hence the avalanche clusters are DP-like, and not affected by the conservation law.

14. Open problems

Let me conclude by discussing some of the interesting open problems in this field. The list is necessarily incomplete, and influenced by personal taste and prejudices.

We can start with the problem of directed abelian sandpile models. In this case, we can calculate all the avalanche exponents in all dimensions. However, time-dependent correlation functions in the model have not been studied analytically so far. In particular, the power spectrum of the stochastic outflux of particles subjected to a steady slow input at top layer seems to be an interesting quantity. There is fairly convincing numerical evidence that this power spectrum is $1/f^2$ [89]. It would be useful to establish this theoretically.

For the undirected BTW model in two dimensions, the most obvious unsolved question is determination of avalanche exponents. Insights from the logarithmic conformal field theory should be useful here [90]. We mentioned earlier that the result that the chemical distance exponent for spanning trees in two-dimensions is 5/4 comes from its connection to the Potts model, and conformal field theory. The spanning trees problem is a rather classical problem in graph theory, but the direct combinatorial proof of this result using the equivalence between the spanning trees and the dimer covering problem on the square lattice is quite recent [91]. One would also like to have similar results in higher dimensions. More generally, most of the papers in literature about spanning trees deal with the number of trees of specified local structure (some specified edges absent, or present). However, questions about the large-scale geometrical structure of spanning trees are not so well studied [92].

Several other questions about the two-dimensional model are rather intriguing, and are not understood yet. One is the structure of the unique recurrent state which corresponds to the identity element of the abelian group. This shows interesting structures, at several length scales, and is not understood. Some good pictures may be found in [93]. Similar structures are seen if the BTW model is relaxed from special unstable states (like all heights 5 [94]). Similarly, we can consider BTW model, with initial height zero everywhere, and add particles only at the origin. As time evolves, the diameter of the region of space reached by the added grains increases as $t^{1/2}$. However, the asymptotic shape of this region is not circular. If we grow the pile in a background of all heights 1, or on a chessboard pattern with half the sites of height 0 and half of height 1, the shape is also not circular, but a different shape. In fact, this appears to be a good example to study how complex patterns can be generated using very simple evolution rules [95].

There is some interest in understanding avalanche exponents on fractals [96]. The main reason for the interest is that one can hope to use exact real-space renormalization group techniques. It turns out that abelian property is preserved under renormalization, but so far application of renormalization group techniques to SOC has been somewhat ad hoc [97].

For $d \leqslant 4$, numerical simulations suggest that while avalanche clusters can have nontrivial topology (two arms of propagating avalanche can join to form a ring), the clusters are not very ramified, and the fractal dimension of avalanche clusters is same as space dimension, i.e., number of distinct sites toppled scales as R^d, where R is the linear size of the avalanche. It would be nice to have a proof (or disproof) of this statement.

For the directed ASM, we showed that there is a simple systematic way to exactly compute the probabilities of avalanches of sizes $1, 2 \ldots$. This is not so for undirected models. The fact that one can calculate the probabilities of different heights in the steady state implies that we can calculate $\mathsf{Prob}(s = 0)$. The calculation of $\mathsf{Prob}(s = 1)$ already involves the condition that all the neighbors of the toppled site are strictly below the critical height, which has not been calculated so far.

Sandpile models with stochastic toppling rules have not been studied so much analytically. Even the characterization of recurrent configurations is not always possible. Consider, for example, a version of the Manna's model on the square lattice with the rule that if height exceeds 1, two particles are transferred in opposite directions, with equal probability for the north-south or east-west transfer. In this case, the closure equations for the algebra of a_i's become

$$a_j^2 = \tfrac{1}{2}(a_{j_1}a_{j_3} + a_{j_2}a_{j_4}). \tag{93}$$

One can prove the existence of FSCs in this *stochastic* model. However an analog of the burning test to determine whether a given configuration is recurrent or not, and how it follows from the equations (93) is not known [98].

Also, it has not been proved that the critical exponents of the undirected Manna model are different from the deterministic case, though the numerical evidence it favor of this is quite strong, and for the directed model, the presumably exact values of exponent are known, and different from the deterministic case [99]. In general, the question of universality classes of the sandpile models is still open. The intriguing relationship between the Manna model and the Anderson localization problem [74] also has not been much explored. The relation of the avalanche propagation to propagation of infection in contact process with many absorbing states is also not quite settled yet [100].

It is hoped that some of the readers will try to seek answers to some of these questions.

References

[1] Available at arXiv.org/abs/cond-mat/9909009.
[2] B.B. Mandelbrot, Fractals: Form, Chance and Dimension, Freeman, San Fransisco, 1977.
[3] A good introduction to various scaling laws in river-networks and references to earlier literature may be found in P.S. Dodds, D.H. Rothman, Phys. Rev. E 59 (1999) 4865;
P.S. Dodds, D.H. Rothman, Phys. Rev. E 63 (2001) 016115;
P.S. Dodds, D.H. Rothman, Phys. Rev. E 016116 (2001); P.S. Dodds, D.H. Rothman, Phys. Rev. E 016117 (2001). See also
F. Colaiori, A. Flammini, A. Maritan, J.R. Banavar, Phys. Rev. Lett. 78 (1997) 4522;
J.R. Banavar, F. Colaiori, A. Flammini, A. Rinaldo, J. Stat. Phys. (2001) 1.
[4] B. Gutenberg, C.F. Richter, Ann. Geophys. 9 (1956) 1;
P. Bak, K. Christensen, L. Danon, T. Scanlon, Phys. Rev. Lett. 88 (2002) 178501.
[5] O. Peters, C. Hertlein, K. Christensen, Phys. Rev. Lett. 88 (2002) 018701.
[6] K.R. Sreenivasan, Ann. Rev. Fluid Mech. 23 (1991) 539–604.
[7] P. Bak, C. Tang, K. Wiesenfeld, Phys. Rev. Lett. 59 (1987) 381.
[8] The actual behavior of real sand is more complicated than this rather idealized description. Our concern here is to provide a physical motivation for the mathematical model. For a recent discussion of more realistic models of granular media, see H.J. Herrmann, Physica A 263 (1999) 51.
[9] P. Bak, How Nature Works, Oxford University Press, Oxford, 1997.
[10] R. Dickman, M.A. Munoz, A. Vespignani, S. Zapperi, Brazilian J. Phys. 30 (2000) 27.
[11] E.V. Ivashkevich, V.B. Priezzhev, Physica A 254 (1998) 97.
[12] D. Dhar, Physica A 263 (1999) 4.
[13] D.L. Turcotte, Rep. Prog. Phys. 62 (1999) 1377.
[14] F. Redig, Les Houches Lectures, preprint, 2005.
[15] A. Dhar, D. Dhar, Phys. Rev. E 55 (1997) R2093;
H. Agrawal, D. Dhar, Phys. Rev. E 63 (2001) 056115;
G.F. Lawler, Intersections of Random Walks, Birkhauser, Boston, 1996.
[16] H. Takayasu, Phys. Rev. Lett. 63 (1989) 2563.
[17] Models of this type were studied earlier by R. Burridge, L. Knopoff, Bull. Seismol. Soc. Am. 57 (1967) 341;
J.M. Carlson, J.S. Langer, Phys. Rev. A 40 (1989) 6470;
M. de Sousa Vieira, Phys. Rev. A 46 (1992) 6288;
M. Paczuski, S. Boettcher, Phys. Rev. Lett. 77 (1996) 111.
[18] H. Flybjerg, Physica A 340 (2004) 552;
K. Sneppen, Phys. Rev. Lett. 69 (1992) 3539;
P. Grassberger, Y.C. Zhang, Physica A 224 (1996) 169;
M. Paczuski, D. Hughes, Physica A 342 (2004) 158.
[19] In fact, we may assume that at each toppling, the assignment of which grain goes to which neighbor is done randomly, then the path of each grain from the point of addition to the boundary is a random walk. In this case, the above bound can be improved to $\langle s \rangle \sim L^2$, which is actually an optimal bound.
[20] V. Frette, K. Christensen, F.J. Malthe-Sorenssen, T. Jossang, P. Meakin, Nature 379 (1996) 49.
[21] G. Grinstein, in: A. McKane, M. Droz, J. Vannimenus, D. Wolf (Eds.), Scale Invariance, Interfaces and Non-equilibrium Dynamics, NATO ASI Series, vol. 344, Plenum, New York, 1995, p. 261.
[22] C. Maes, F. Redig, E. Saada, Commun. Math. Phys. 244 (2004) 395.
[23] A. Corral, M. Paczuski, Phys. Rev. Lett. 83 (1999) 572.
[24] "My name means the shape I am- and a good handsome shape it is too. With a name like yours, you might be any shape, almost."- Humpty Dumpty to Alice in Through the Looking Glass by Lewis Carroll.
[25] D. Dhar, Phys. Rev. Lett. 67 (1990) 1613.
[26] R. Meester, F. Redig, D. Znamenski, Markov Proc. Rel. Fields 7 (2001) 509–523.
[27] B. Drossel, F. Schwabel, Phys. Rev. Lett. 69 (1992) 1629.
[28] Y.C. Zhang, Phys. Rev. Lett. 63 (1989) 470.
[29] D. Dhar, P. Ruelle, S. Sen, D.N. Verma, J. Phys. A 28 (1995) 805.
[30] N. Jacobson, Basic Algebra, Freeman, San Fransisco, 1974.
[31] This procedure is equivalent to the script test first proposed in Speer E. R., J. Phys. A 71 (1993) 61.
[32] S.N. Majumdar, D. Dhar, Physica A 185 (1992) 129.
[33] C.M. Fortuin, P.W. Kasteleyn, Physica 57 (1972) 536.
[34] L.C. Merino, Ann. Comb. 1 (1997) 253;
R. Cori, Y. Le Borgne, Adv. Appl. Math. 30 (2003) 44.
[35] For a recent treatment of this classical result, see F.Y. Wu, Rev. Mod. Phys. 54 (1982) 235.
[36] H. Saleur, B. Duplantier, Phys. Rev. Lett. 58 (1987) 2325;
A. Coniglio, Phys. Rev. Lett. 62 (1989) 3054.
[37] F. Harary, Graph Theory, Addison-Wesley, Reading, MA, 1990.

[38] E.V. Ivashkevich, D.V. Ktitarev, V.B. Priezzhev, Physica A 209 (1994) 347.
[39] D. Dhar, S.S. Manna, Phys. Rev. E 54 (1994) 2684.
[40] F. Spitzer, Principles of Random Walk, Van Nostrand, Princeton, 1964.
[41] A.Z. Broder, in: Proceedings of the 30th Annual IEEE Symposium on Foundations of Computer Science, IEEE, New York, 1989, p. 442.
[42] S.N. Majumdar, Phys. Rev. Lett. 68 (1992) 2329.
[43] D. Dhar, R. Ramaswamy, Phys. Rev. Lett. 63 (1989) 1659.
[44] D. Dhar, in: J. Pati, Q. Shafi, S. Wadia, Yu Lu (Eds.), Current Trends in Condensed Matter, Particle Physics and Cosmology, World Scientific, Singapore, 1990, p. 117.
[45] W. Feller, An Introduction to Probability Theory and Its Applications, Wiley, New York, 1970.
[46] T. Jonsson, J.F. Wheater, J. Stat. Phys. 92 (1998) 713.
[47] S. Lubeck, Phys. Rev. E 58 (1998) 2957.
[48] P. Ruelle, S. Sen, J. Phys. A 25 (1992) 1257.
[49] A.A. Ali, D. Dhar, Phys. Rev. E 51 (1995) R2705;
    A.A. Ali, D. Dhar, Phys. Rev. E 52 (1995) 4804.
[50] D. Dhar, S.N. Majumdar, J. Phys. A 23 (1990) 4333.
[51] G.W. Peng, J. Phys. A 25 (1992) 5279.
[52] C. Tang, P. Bak, J. Stat. Phys. 51 (1988) 797;
    B. Gaveau, L.S. Schulman, J. Phys. A 24 (1991) L475;
    S.A. Janowski, C.A. Laberge, J. Phys. A 26 (1993) L973;
    H. Flybjerg, Phys. Rev. Lett. 76 (1996) 940.
[53] S.N. Majumdar, D. Dhar, J. Phys. A 24 (1991) L357.
[54] V.B. Priezzhev, J. Stat. Phys. 74 (1994) 955;
    See also V.B. Priezzhev, Physica Scripta T49B (1993) 663.
[55] P. Grassberger, private communication.
[56] G. Piroux, P. Ruelle, Phys. Lett. B 607 (2005) 188.
[57] S.S. Manna, Physica A 179 (1991) 249;
    K. Christensen, Z. Olami, Phys. Rev. E 48 (1993) 3361;
    S. Lubeck, K.D. Usadel, Phys. Rev. E 55 (1997) 4095;
    A. Chessa, E. Marinari, A. Vespignani, S. Zapperi, Phys. Rev. E 57 (1998) 6241.
[58] V.B. Priezzhev, E.V. Ivashkevich, D.V. Ktitarev, Phys. Rev. Lett. 76 (1996) 2093.
[59] D.V. Ktitarev, V.B. Priezzhev, Phys. Rev. E 58 (1998) 2883.
[60] M. De Menech, A.L. Stella, C. Tebaldi, Phys. Rev. E 58 (1998) R2677 [cond-mat/9805045].
[61] C. Tebaldi, M. De Menech, A.L. Stella, Phys. Rev. Lett. 83 (1999) 3952.
[62] E.V. Ivashkevich, D.V. Ktitarev, V.B. Priezzhev, J. Phys. A 27 (1994) L585.
[63] M. Paczuski, S. Boettcher, Phys. Rev. E 56 (1997) R3745.
[64] D.V. Ktitarev, S. Lubeck, P. Grassberger, V.B. Priezzhev, Phys. Rev. E 61 (2000) 81.
[65] H. Agrawal, D. Dhar, Phys. Rev. E 63 (2001) 056115 [cond-mat 0012102].
[66] V.B. Priezzhev, J. Stat. Phys. 98 (2000) 667 [cond-mat 9904054].
[67] A.E. Scheidegger, Bull. Assoc. Sci. Hydrol. 12 (1967) 15.
[68] E. Somfai, L.M. Sander, Phys. Rev. E 56 (1997) R5;
    S.S. Manna, B. Subramanian, Phys. Rev. Lett. 76 (1996) 3460;
    K. Sinclair, R.C. Ball, Phys. Rev. Lett. 76 (1996) 3360;
    J. Huang, D.L. Turcotte, J. Geophys. Res. 94 (1989) 7491 and references cited therein.
[69] T.M. Liggett, Interacting Particle Systems, Springer, New York, 1985;
    R. Durrett, Lecture Notes on Particle Systems and Percolation, Wadsworth, Belmont, 1988.
[70] V.B. Priezzhev, A. Dhar, D. Dhar, S. Krishnamurthy, Phys. Rev. Lett. 77 (1996) 5079.
[71] R.R. Shcherbakov, V.V. Papoyan, A.M. Povolotsky, Phys. Rev. E 55 (1997) 3686.
[72] R. Shcherbakov, D.L. Turcotte, Physica A 277 (2000) 274.
[73] S.S. Manna, J. Phys A 24 (1991) L363.
[74] P.A. Lee, T.V. Ramakrishnan, Rev. Mod. Phys. 57 (1997) 287.
[75] A.A. Ali, Phys. Rev. E 52 (1995) R4595.
[76] S. Maslov, C. Tang, Y.-C. Zhang, Phys. Rev. Lett. 83 (1999) 2449–2452.
[77] J. Kertesz, L.B. Kiss, J. Phys. A 23 (1990) L433.
[78] L. Laurson, M.J. Alava, S. Zapperi, J. Stat. Mech.; Theo. Exp. (2005) L11001.
[79] D. Dhar, Physica A 340 (2004) 535.
[80] K. Christensen, A. Corral, V. Frette, J. Feder, T. Jossang, Phys. Rev. Lett. 77 (1996) 107.
[81] D. Dhar, P. Pradhan, J. Stat. Mech: Theo. Exper. 1 (2004) P05002 [cond-mat/0404019].
[82] P. Pradhan, D. Dhar, to appear in Phys. Rev. E (2006) [cond-mat/051127].
[83] M. Baiesi, C. Maes, preprint 2005 [cond-mat/0505274].
[84] S. Boettcher, M. Paczuski, Phys. Rev. Lett. 79 (1997) 889.
[85] A. Ben-Hur, O. Biham, Phys. Rev. E 53 (1996) R1317.

[86] H. Hinrichsen, Adv. Phys. 49 (2000) 815.

[87] M.A. Munoz, R. Dickman, A. Vespignani, S. Zapperi, Phys. Rev. E 59 (1999) 6175.

[88] P.K. Mohanty, D. Dhar, Phys. Rev. Lett. 89 (2002) 104303.

[89] S. Lubeck, K.D. Usadel, Fractals 1 (1993) 1030.

[90] M. Jeng, Phys. Rev. E 71 (2005) 016140;
S. Moghimi-Araghi, M.A. Rajabpour, S. Rouhani, Nucl. Phys. B 718 (2005) 362.

[91] R. Kenyon, Act. Math. 185 (2000) 239 [math-ph/0011042].

[92] S.S. Manna, D. Dhar, S.N. Majumdar, Phys. Rev. A 46 (1992) R4471.

[93] M. Creutz, Comput. Phys. 5 (1991) 198.

[94] S.H. Liu, T. Kaplan, L. Gray, Phys. Rev. A 42 (1990) 3207.

[95] S. Ostojic, Physica A 318 (2003) 187.

[96] B. Kutnjak-Urbanc, S. Zapperi, S. Milosevic, H.E. Stanley, Phys. Rev. E 54 (1996) 272;
F. Daerden, C. Vanderzande, Physica A 256 (1998) 533.

[97] L. Pietronero, A. Vespignani, S. Zapperi, Phys. Rev. Lett. 72 (1994) 1690;
J. Hasty, K. Wiesenfeld, J. Stat. Phys. 86 (1997) 1129.

[98] D. Dhar, Physica A 270 (1999) 69 [cond-mat 9902137].

[99] M. Paczuski, K. Bassler, Phys. Rev. E 62 (2000) 5347;
M. Kloster, S. Maslov, C. Tang, Phys. Rev. E 63 (2001) 026111.

[100] R. Dickman, A. Vespignani, S. Zapperi, Phys. Rev. E 57 (1998) 5095;
A. Vespignani, R. Dickman, M.A. Munoz, S. Zapperi, Phys. Rev. Lett. 81 (1998) 5676.